PRECIPITATION, PLANT COMMUNITIES AND METHANE FLUXES IN THE KA`AU CRATER WETLAND, O`AHU, HAWAI`I

A THESIS SUBMITTED TO
THE GLOBAL ENVIRONMENTAL SCIENCE
UNDERGRADUATE DIVISION IN PARTIAL FULFILLMENT
OF THE REQUIREMENTS FOR THE DEGREE OF

BACHELOR OF SCIENCE

IN

GLOBAL ENVIRONMENTAL SCIENCE

DECEMBER 2003

By

Maxime Grand

Thesis Advisor:

Eric Gaidos

I certify that I have read this thesis and that, in my opinion, it is satisfactory in scope and quality as a thesis for the degree of Bachelor of Science in Global Environmental Science.

THESIS ADVISOR

_____

Eric Gaidos
Department of Geology & Geophysics

Acknowledgements

I would like to thank Aly El-Kady and Bob Whittier for providing the water level sensor necessary for this study. I would like to express my appreciation to the Board of Water Supply for granting access to the Ka`au crater for this research. The NOAA Hawaii Sea Grant Global Environmental Science Fellowship for Senior Thesis Research partly funded this research and allowed to present my results at the Fall 2003 AGU meeting. I am grateful for all the assistance provided by Angelos Hannides and all GES and G&G undergraduate students that helped me carry both chambers to the crater. Finally, I would especially like to thank my advisor, Eric Gaidos, for his support, timely meetings, help in the field and for the wonderful undergraduate experience he has provided me.

Abstract

Methane emissions from the Ka`au crater tropical wetland on the island of O`ahu were monitored from August to November 2003. Net methane emission was measured using static chambers and the methane production and oxidation potentials of soil samples were assayed. Environmental parameters (water table level, precipitation, temperature and Photosynthetically Active Radiation (PAR)) were also measured. In addition, the organic chemical composition in different soils was measured.

Average net methane emissions varied considerably among different vegetation patterns in the wetland, ranging between 17 and 160 mg m^{-2} day^{-1}. Considering the area covered by each pattern, the average net methane flux from the crater is 84 ± 4 mg m^{-2} day^{-1}. Methane production potentials ranged between $6*10^{-6}$ and $1*10^{-3}$ mg $g(dry\ soil)^{-1}$ day^{-1}. Methane oxidation potentials were approximated using first order reaction kinetics and ranged between 0.08 and 0.026 hr^{-1} $g(dry\ soil)^{-1}$.

Water table level was found to be the main environmental parameter influencing net methane emissions, affecting primarily the methane generation potential of soil samples. Methane oxidation potentials were mostly affected by ambient methane concentrations. The variation in methanogenic activity due to the ± 0.05°C temperature variation recorded in the soil throughout the sampling period was calculated to be 0.07%, much less than the observed variation in net emission and methane generation potentials. No correlation was observed between net methane emissions and PAR. Moreover, the soil organic carbon content was similar among three of the five vegetation patterns studied.

Past changes in vegetation suggest that methane emissions may have decreased since the early 1900s. This trend is expected to prevail in the future if the vegetation patterns contributing the least to the overall methane flux spread. Additionally, anthropogenic

greenhouse warming is likely to reduce precipitation in Hawaii during this century which may in turn reduce the net methane emissions from the Ka`au crater wetland even further.

Table of Contents

List of Tables

List of Figures

1. INTRODUCTION

1.1 Methane, an Important Greenhouse Gas

Methane (CH_4) is a potent greenhouse gas which plays a major role in atmospheric chemistry. Methane is the second most important radiatively active gas after CO_2. The contribution of methane to the greenhouse effect is minor relative to CO_2 because of its small atmospheric concentration (1.75 ppm) but methane is 25 times stronger than CO_2 at trapping long wave infrared radiation. Also, the yearly rate of accumulation of CH_4 in the troposphere is greater than CO_2. Methane is also involved in the production of tropospheric ozone, itself a very potent greenhouse gas (Milich, 1999). Ice core records from Greenland have shown that changes in methane concentrations over time are coincident with climate change, e.g., the termination of the Younger Dryas cold interval 11,600 years before present (Severinghaus et al., 1998).

Once released to the troposphere, methane has a mean residence time of 9 years before being oxidized by hydroxyl radicals (OH^-):

$$CH_4 + OH\bullet \rightarrow CH_3\bullet + H_2O$$

OH oxidation of methane amounts for 94% of all CH_4 sinks while oxidation in upland soils amount for the remaining 6% (Le Mer and Roger, 2001).

Anthropogenic sources such as biomass and fossil fuel burning, rice paddies and livestock farming, domestic sewage, landfills and natural gas pipeline leaks are now responsible for 60% or more of methane emissions (Mackenzie, 1998). Recent estimations of methane annual emission by the International Panel for Climate Change (IPCC) were 300 Tg for the year 2000 and between 400-600 Tg for 2010 (IPCC, 2000).

Methane may therefore play an increasingly important role in climate change during this century.

1.2 Methane and Natural Wetlands

Wetlands account for 21% of all the methane emissions to the atmosphere. Tropical wetlands such as Ka`au crater account for 55% of all wetland emissions (Prather et al., 1995). The global average net methane flux from tropical wetlands to the atmosphere is 50-137 mg m^{-2} yr^{-1} (Schlesinger, 1997). Assessing global emissions rates from natural wetlands is a difficult task because local methane emissions in wetlands can vary significantly over a few meters (IPCC, 2001). Consequently, net methane fluxes from natural wetlands are subject to large uncertainties.

Rice paddies, boreal and subarctic mires and temperate wetlands have been extensively studied (Wang et al., 1999; Kettunen et al., 1999; Le Mer and Roger, 2001; Öquist and Svensson, 2002). Methane emission from natural tropical wetlands have been less investigated and the fluxes reported are restricted in geographical coverage (Bartlett and Harriss, 1993). Therefore, studies of wetlands and especially those in a tropical setting are of great significance due to their large contribution to global methane emissions and the lack of net methane emission data from the tropics.

1.3 Methane Production, Consumption and Net Emission in Wetland Soils

Most atmospheric methane is of biological origin (Le Mer and Roger, 2001). In a tropical setting, primary production often exceeds oxidative degradation, leaving an excess organic matter pool available to methanogens (Miyajima et al., 1997). In wetland sediments, methane is produced by methanogenic Archea under strict anoxic conditions and low concentrations of sulfate and nitrate. Competitive interactions with nitrate and sulfate-reducing bacteria limit the availability of organic matter for methanogens (Le Mer and Roger, 2001). Methanogenic Archea produce methane primarily by the breakdown of acetate, a product of fermentative decomposition:

$$CH_3COOH \rightarrow CH_4 + CO_2$$

Methane can also be generated by CO_2 reduction:

$$CO_2 + 4H_2 \rightarrow CH_4 + 2H_2O$$

Soil redox potential (Eh) is probably the most important constraint on methane production. A redox potential lower than –150mV is the ultimate prerequisite for the production of CH_4 in any soil (Wang et al., 1999). Above the –150mV threshold, soil organic matter is converted to CO_2 and the methanogenic community is inactive.

The second sink of methane after oxidation by hydroxyl radicals in the atmosphere is the aerobic oxidation of methane to CO_2 in soils by methanotrohic bacteria. Two types of methane oxidation have been identified. High affinity oxidation occurs at concentrations of methane < 12 ppm whereas low affinity oxidation is performed under CH_4 concentrations > 40 ppm. The bacterial community involved in high affinity oxidation has not yet been identified. The consumption of methane in methanogenic

environments such as wetlands, rice fields and landfills is a low affinity oxidation (Le Mer and Roger, 2001). In freshwater wetland soils, high affinity methanotrophic activity can be neglected due to high ambient methane concentrations (Bodegom et al., 2001).

Methanotrophic bacteria are found at anaerobic-aerobic soil interfaces and in plant root systems. Recent investigations have also found methanotrophs associated with leaves and stems of vascular plants (Heilman and Carlton, 2001). Methane is their only carbon source and the availability of oxygen limits their activity (Le Mer and Roger, 2001; Bodegom et al., 2001). As methanonotrophy requires both a constant methane supply and oxic conditions, methanotrophic populations develop where high methane and oxygen concentrations overlap in the soil profile (Kettunen et al., 1999). The consumption of CH_4 by methanotrophs balances the production of CH_4 by methanogens and regulates the overall CH_4 flux from wetland soils. In rice field soils, it has been estimated that more than 90% of the CH_4 generated under anaerobic conditions at depth can be re-oxidized in the oxic zone of the soil (Le Mer and Roger, 2001). The same observation was made in the Florida Everglades (King et al, 1990).

At any time, the total flux of methane escaping a wetland is equal to the amount of methane produced by methanogens at depth minus the amount of methane oxidized by the methanotrophs:

Net CH_4 Flux= F(methane production)- F(methane oxidation)

As shown in Fig. 1, the CH_4 produced in wetland soils can escape to the atmosphere through diffusion, ebullition and passive transport through plant lacunae (air spaces forming channels in leaves, stems and roots). When the soil is submerged and the concentration of dissolved methane in the soil is large enough, bubbles of gas can form,

migrate to the surface, and escape to the atmosphere. When the water table level is below the surface, CH_4 can be released to the atmosphere by diffusion through sediment pores. Many wetland plants have hollow stems composed of aerenchyma, a spongy tissue with large air spaces. This property allows them to act as gas conduits from the soil to the atmosphere. The methane produced in the soil diffuses through plant roots and conductive tissues (i.e. stem and stomata) and is then released to the atmosphere. Generally, sites colonized with plants with an aerenchyma have higher rates of methane release due to internal CH_4 transport (Le Mer and Roger, 2001). Thus, plant stems can provide a direct gas transportation pathway allowing methane to migrate from root systems to the atmosphere, avoiding surface oxidation zones (Öquist and Svensson, 2002). The same pathway also provides a mean for oxygen to reach anaerobic environments supporting communities of methanotrophs.

In summary, in wetland soils net methane emission reflects the balance between methanogenesis and methanotrophy. Three pathways allow methane to escape to the atmosphere: ebullition when the soil is submerged, diffusion through soil pores and transport through plant conductive tissues.

1.4 Influence of Environmental Parameters and Vegetation on CH_4 Emissions

Net methane emissions from wetland soils are strongly regulated by environmental parameters such as precipitation, water table level, temperature, soil chemical composition and Photosynthetically Active Radiation (PAR). In addition, plant communities can influence the magnitude of the methane fluxes in wetland ecosystems (Öquist and Svensson, 2002).

Water Table Level

Water table level is probably the most important parameter regulating net methane emissions from wetland soils (Öquist and Svensson, 2002; Sahagion and Melack, 1996). Waterlogged soils are prone to anoxia at depth, the main requirement for methanogenesis to occur. A water layer covering a wetland soil reduces the oxygen exchange between the atmosphere and the sediment. If the soil is flooded for a sufficient period of time, the consumption of oxygen becomes greater than the atmospheric re-supply. Eventually, the soil becomes completely anoxic. Soil submersion will also reduce the activity of methanotrophs by lowering the availability of oxygen in it. Conversely, when the water table level lies below the soil surface the diffusion of oxygen is enhanced which increases the width of the oxidized soil layer hosting methanotrophs and decreases the width of the reduced soil layer hosting methanogens (Le Mer and Roger, 2001). Therefore, water table level fluctuations regulated by precipitation, evaporation and drainage can considerably affect methane emissions in wetland soils. In addition to the effects of soil moisture on oxygen concentrations, water table level fluctuations may affect the amount of organic matter available to methanogens. When the water table level declines, increased aerobic degradation reduces the amount of organic matter that would promote methanogenesis in anoxic conditions (Kettunen et al., 1999).

Soil Texture

Net methane emissions are also dependant on the texture of the soil. Soil texture is involved in the establishment of anaerobic conditions required for methanogenesis, in the transfer of the CH_4 produced at depth towards the surface and in the width of the aerobic surface layer where methanotrophy occurs (Le Mer and Roger, 2001). Therefore,

depending on the soil texture, net methane emissions from wetlands can be reduced or enhanced. Soils with a high gas diffusion coefficient can develop a wide oxidized layer hosting methanotrophs and net methane emission is decreased. On the other hand, poorly drained soils such as clay soils with a slow gas diffusion rate have a smaller oxidized layer and a large reduced layer hosting methanogens allowing higher net methane emissions. A slow gas diffusion rate may also delay the net methane emission response to fluctuations in environmental parameters.

Temperature

Methane production is optimum between 30 °C and 40 °C. On the other hand, large temperature variations do not affect methane consumption rates (Le Mer and Roger, 2001). In tropical wetlands, temperature is nearly optimal for methanogenesis throughout the year (25 °C to 35 °C). (Le Mer and Roger 2001, Miyajima et al. 1997). Some scholars argue that temperature is a less important variable compared to water table level variations in tropical wetlands (Sahagion and Melack, 1996).

Vegetation

Methane emission may vary with dominant plant type. Some wetland plants have aerenchyma tissues while others do not. Le Mer and Roger (2001) state that plants without aerenchyma cells decrease methane emission because more methane is oxidized in the rhizosphere and plant mediated methane transport is reduced. Furthermore, the organic matter content of the soil may differ from one vegetation pattern to the other and may thus affect methane generation. By comparing methane fluxes from two vegetation patterns in a subarctic mire, Öquist and Svensson (2002) showed that one set of plants induced higher methane emissions by increasing the amount of organic matter available

to methanogens in the soil while the other pattern also increased methane emission by facilitating the transportation of CH_4 from the soil to the atmosphere. In a wetland with various vegetation patterns, net methane emission may thus vary considerably from one pattern to the other.

Photosynthetically Active Radiation

Photosynthetically Active Radiation (PAR) is another parameter that may affect net methane emissions. When the PAR is high, the plant stomata are more open, enhancing transport of oxygen and methane. On the contrary, when the PAR is low, stomatal conductance is reduced as well as oxygen and methane transport.

1.5 Study Area: Ka`au Crater

Ka`au crater is a ~ 650,000 year old post-erosional explosion vent of the Honolulu Volcanic Series (Mac Donald et al., 1983). It is located on the leeward side of the Ko`olau Range at the head of the Palolo valley, southeastern O`ahu (21°20'00" N, 157°46'30" W) (Fig.2). The crater is approximately 500 m in diameter at an elevation of 463 m. It is bounded by a portion of the Ko`olau Range (elevation 700 m) on its northeast side and by the crater rim elsewhere. Surface drainage in the crater occurs through a single outlet, through a notch in the crater rim on the southeast side into a stream that falls 144 meters to join Waiamao Stream in Palolo Valley (Fig. 3).

Ka`au Crater experiences a subtropical climate with constant northeast trade winds prevailing throughout the year. The average temperature is 21 °C ± 2 °C (Armstrong, 1983). As a result of this stable climate, the confusing effects of temperature on methane emissions in Ka`au Crater will be negligible. At the Palolo Valley rain gauge

located 160 meters below the crater's floor, annual precipitation is 3,400mm (Hotchkiss and Juvik, 1999).

The crater's vegetation has changed over time with a shift from an `ohi`a forest to wetland-adapted species such as sedges and reeds. At the beginning of the 20th century, the crater was half covered with an `ohi`a forest that has gradually decreased in size. According to Kennedy (1975), the recession of the `ohi`a forest may be due to an attempt to transform the crater into a reservoir in the early 1900's. The reservoir may have drowned the root systems of large trees and facilitated the colonization of a part of the `ohi`a forest by low-oxygen tolerant species. Kennedy (1975) identified five major vegetation patterns in the crater: `ohi`a scrub, strawberry guava forest, honohono meadow, sedge meadow and ti thicket (Fig.3). These patterns are still identifiable today. A comparison of aerial photos from 1952 to 1969 suggests that the `ohi`a scrub is being replaced by the sedge meadow while the Strawberry Guava forest is increasing in size near the outlet point (Kennedy, 1975). The invasion of the strawberry guava may be facilitated by seed dispersion by feral pigs and from soil trapping by strawberry guava roots.

The crater soil is composed of a top layer of peat overlying a layer of clay (Kennedy, 1975). Although the crater floor seems relatively flat, the water table level relative to the surface fluctuates from one location to the other, probably because of some micro-topographic variations. For example, the strawberry guava canopy soil is often drier than the sedge and honohono meadows. However, in general the soil is waterlogged and often covered by water.

The Ka`au crater wetland is a unique site that is geographically, geologically and hydrologically well defined. It lies within a watershed management area run by the Honolulu Board of Water Supply and is relatively undisturbed by human activities. It is accessible by trail in less than two hours from parking in Palolo Valley.

1.6 Research Objectives

The primary goals of this project are to: (1) measure net methane emission in Ka`au crater, (2) investigate the influence of environmental parameters (water table level, PAR, temperature and organic chemical composition) and vegetation on net methane emissions, (3) understand the patterns of net emission in terms of methane production and oxidation potentials of the soil.

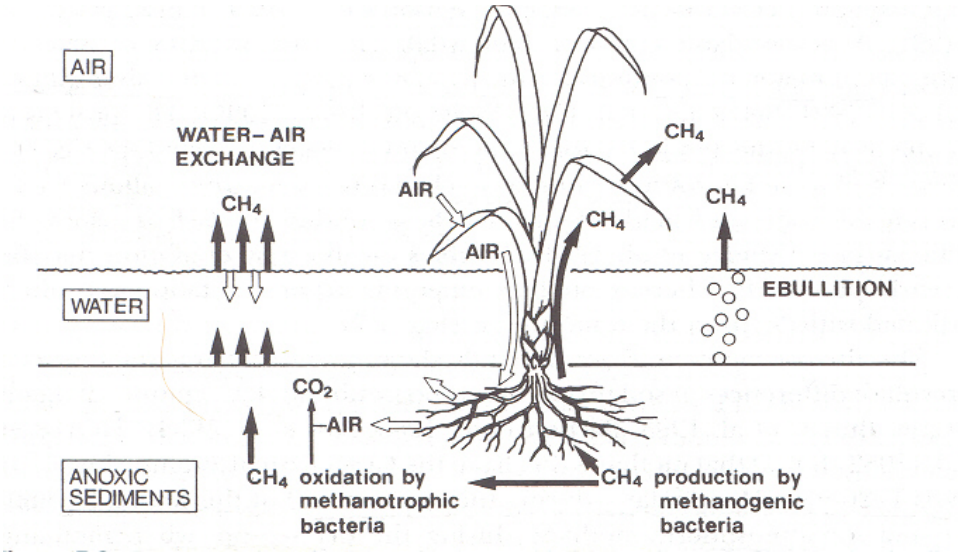

Figure 1. Methane production, oxidation and release pathways to the atmosphere From Schütz et al. (1991)

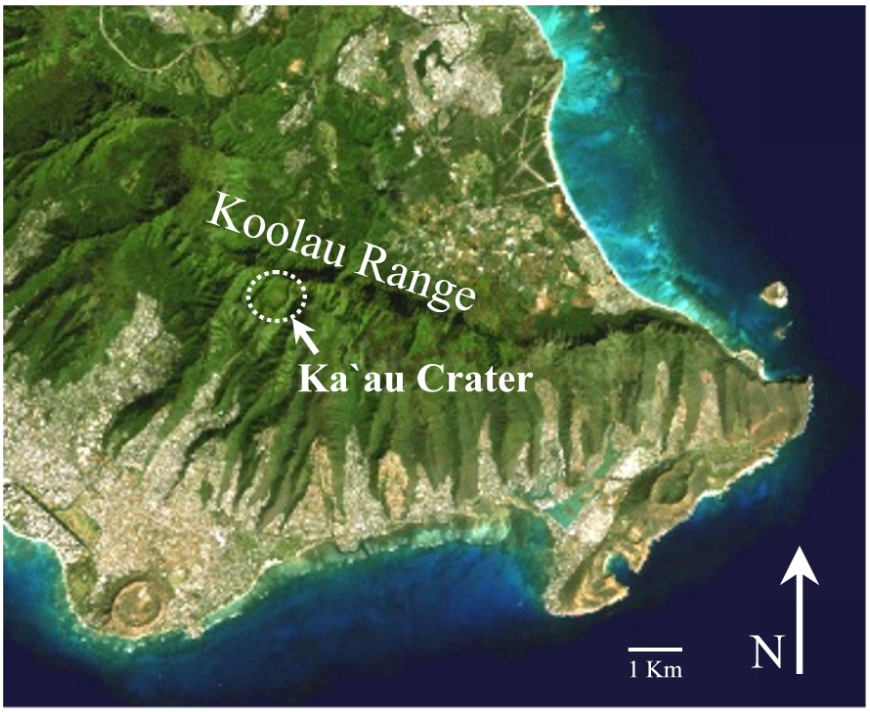

Figure 2. Satellite image of southeatern Oahu showing Ka`au Crater Location

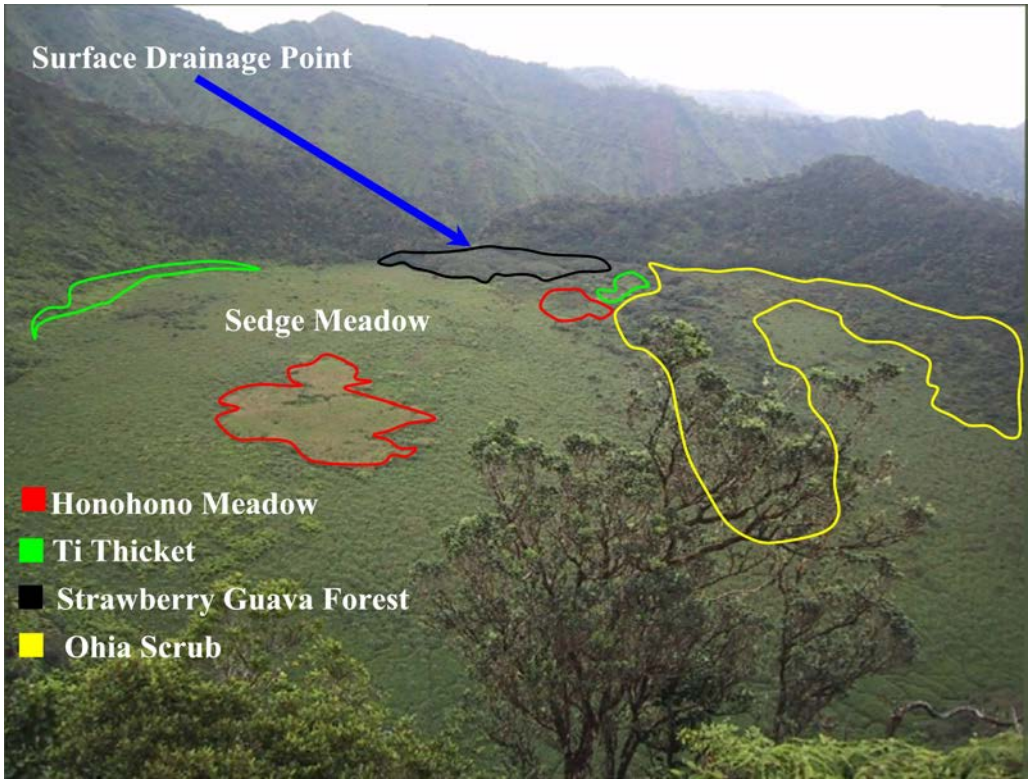

Figure 3: General view of Ka`au Crater physical features and vegetation patterns

2. MATERIALS AND METHODS

2.1 Methane

2.1.1 Net Methane Emission

The net methane flux from the Ka`au crater wetland was measured using two 210 L static chambers covering 0.25 m^2 of the swamp. The chambers were made with two translucent polyethylene buckets and their lids. Large buckets were used to allow the insertion of plants within the chambers without having to trim them. A 0.125 m^2 hole was cut in the middle of each lid and galvanized roof flashing was attached around it. The modified lid constitutes the bottom part of each chamber (i.e., the collar), which was inserted into the wetland soil (Fig.4). To avoid stratification of gas concentrations within the chambers, a computer fan powered by a 9V battery was mounted on each collar. Once the collar was properly placed into the soil, the fan was started and the polyethylene bucket was fit to the top of the collar. Air samples were taken through a butyl rubber stopper at the top of the chambers using a 20 mL syringe. Each sample was then injected into a previously evacuated 10 mL serum bottle and returned to the lab for subsequent analysis. By injecting 20 mL of sample into a 10 mL bottle, a positive pressure gradient was maintained between the sample and ambient air.

For each measurement, a chamber was deployed for 2 hours. Using the average global tropical wetland methane flux derived from Schlesinger (1997), it was estimated that a 2-hour incubation time would be adequate to acquire methane concentrations above our detection limit (0.25 ppm see section 2.1.1). Gas samples were obtained at t=0, 15, 30, 60, 90 and 120 minutes. At the beginning of each incubation, an ambient air sample was also taken.

All the static chamber flux measurements were performed weekly between day 242 and day 306 in 2003. From day 264 to 306 the two chambers were used simultaneously in two different vegetation patterns. One of the chambers was deployed in the honohono meadow pattern defined by Kennedy (1975) for the whole period. The second chamber was deployed each time in a different vegetation pattern (i.e., in the strawberry guava canopy, sedge meadow, `ohi`a scrub and ti thicket). Using two chambers simultaneously allows the net methane emission from different vegetation patterns to be compared at the same time and under similar conditions (temperature, water table and PAR). On day 291, both chambers were deployed 2 meters away from each other in the honohono meadow to compare and measure twice the methane flux recorded by each chamber. This was done to assess the repeatability of each measurement and to determine the amount of variation within a vegetation pattern. Table 1 and Fig. 5 summarize the static chamber sampling schedule and the location of the experiments respectively.

2.1.2 Gas Analysis

All the air samples in this study were analyzed using a SRI 310C gas chromatograph (GC) equipped with a flame ionization detector (FID) and an Altech Hayesep T 801100 column (5'x 1/8''x 0.85'') with Helium (He) as a carrier gas. The column temperature was set at 32 °C and the injection and detector temperatures were set at 136 °C. The helium flow to the GC was set at 30 psi, hydrogen at 20 psi and air at 8 psi. The GC was hooked to a laptop computer and all the peak areas resulting from the injection of a sample were integrated using the software Peak Simple 2000.

For every experiment, the GC standardization was performed by injecting 0.5 mL of a 100 ppm methane standard using an SGE gas tight syringe. Standard injection was repeated until the peak areas calculated by Peak Simple agreed within 2% before, during and after each run. For each analysis, the overall standard was calculated by averaging all standard injections. For each experiment, each air sample injected was 0.5 mL.
The GC repeatability was measured by injecting 20 ambient air samples in the GC and by calculating the average and standard deviation of the results. The GC sensitivity is approximately 0.25 ppm for ambient air methane concentrations.

2.1.3 Net Methane Flux Calculations

The CH_4 concentration (in ppm) at any time in the chamber was calculated using:

$$C(t) = \frac{AU(t) \times 100\ ppm}{AU_{100}}$$

where, AU(t) is the average peak areas of two replicates of an air sample withdrawn from the chamber at time t in Arbitrary Units (AU) and AU_{100} is the average peak area in Arbitrary Units of the100 ppm standards injected into the GC for the experiment.

The net methane escaping the soil in each vegetation pattern was calculated according to the following equation**:**

$$F(mg(CH_4)\ m^{-2} day^{-1}) = \frac{\Delta C \times V \times P \times \mu \times 12}{1000 \times R \times T \times A}$$

where, F is the methane emission rate, ΔC is the CH_4 concentration difference between t=2hours and t=0 in the chamber in ppm ($\Delta C = C(CH_4)_{t=2hrs} - C(CH_4)_{t=0}$), V is the volume

of the chamber (0.2082 m^3), μ is the molar mass of methane (16g/mol), P is the atmospheric pressure in Pascals (101,325 Pa), R is the ideal gas constant (8.3145 J/mol/K), T is the temperature in Kelvins (298.15 K) and A is the area of swamp covered by the chamber (0.25 m^2).

For each vegetation pattern, (except for the ti thicket and `ohi`a Scrub where only 1 measurement was performed) the net methane fluxes were averaged and their standard deviation and standard error calculated.

2.1.4 Ka`au Crater Daily Average Net Methane Flux

The crater is approximately 500 meters in diameter and assumed to be a circle. Therefore, the area of the crater is approximately 20 ha. The area occupied by each vegetation pattern was estimated using a map made from a 1969 aerial photo of the crater (Kennedy, 1975). In 1969, 43% of the crater floor was occupied by the `ohi`a scrub, 37% by the sedge meadow, 4% by the strawberry guava canopy, 8% by the honohono meadow and 8% by the ti thicket. Hence, at this time, 84,500 m^2 of the crater was covered by the `ohi`a scrub, 72, 700 m^2 by the sedge meadow, 7,900 m^2 by the strawberry guava forest and 15,700 m^2 were covered with the honohono meadow and ti thicket. The average methane flux escaping Ka`au crater was calculated using the following equation:

$$\overline{F}_{Ka`au} = \frac{(F_h \times A_h) + (F_s \times A_s) + (F_{SG} \times A_{SG}) + (F_o \times A_o) + (F_{ti} \times A_{ti})}{A_h + A_s + A_{SG} + A_o + A_{ti}}$$

where, $F_{Ka`au}$ is the overall methane flux escaping Ka`au crater in mg m^{-2} day^{-1}, F_h, F_s, F_{SG}, F_o and F_{ti} are the average net methane fluxes from the honohono meadow, sedge meadow, strawberry guava canopy, `ohi`a scrub and ti thicket respectively in mg m^{-2} day^{-1}, A_h, A_s, A_{SG}, A_o, A_{ti} are the areas of the honohono meadow, sedge meadow, strawberry guava canopy, `ohi`a scrub and ti thicket respectively. The overall methane emission from the Ka`au crater wetland was calculated by multiplying the above equation by the area of Ka`au Crater and was converted to units of metric tons/year.

2.1.5 Soil Methanogenic Potential

Between days 242 and 306, soil samples were collected every week from the surface layer (0-20 cm) next to both chambers. The methanogenic potential of each soil was estimated in the laboratory using a modified version of the method developed by Wang et al. (1999). The samples were placed in 150 mL serum bottles and 0 to 20 mL of water from the crater was added to each to turn the soil into slurries. When the water table level was above the surface, the addition of water into the bottle was often unnecessary. It is assumed that by immediately incubating the soil samples when returning from the field, the measured methane generation reflects the potential activity of methanogens at the time of sampling. Each serum bottle was then closed with a butyl rubber stopper and aluminum crimp seals to allow gas sampling from the headspace. To create anaerobic conditions, the headspace of every bottle was flushed with N_2 for 15 minutes while a magnetic bar stirred the slurries (Wang et al., 1999). After the flush, a sample was withdrawn from the headspace and analyzed using the GC to ensure that the flushing was efficient and that no CH_4 was detected in the headspace. The bottles were

then incubated at constant temperature (21 °C) for 24 hours. After 24 hours, the slurries were stirred again for 15 minutes to release the methane trapped in the soil to the headspace and a gas sample was taken and analyzed.

To measure the exact headspace volume of each bottle, the bottles were weighed, deionized water was added to each of them until overflowing and the bottles were weighted again. The weight difference after and before the addition of DI water was divided by the density of water, giving the headspace volume. The content of each bottle was then poured and air-dried for 2 to 3 weeks and weighed. To accelerate the drying, some samples were air-dried using a convecting oven set at 60 °C.

The headspace CH_4 concentration of each bottle was calculated as follows:

$$C_2(t = 24hrs) = \frac{AU_{24} \times 100\ ppm}{AU_{100}}$$

where C_2 is the headspace CH_4 concentration in ppmv, AU_{24} is the average peak areas of two air samples withdrawn from the headspace after 24 hours in arbitrary units, and AU_{100} is the average peak area of the100 ppm methane standards injected into the GC for the experiment.

The CH_4 production rate potential of the soil was calculated according to the following equation:

$$F_2(mg(CH_4).g(dry\ soil)^{-1}.day^{-1}) = \frac{C \times HS \times P \times \mu}{10^3 \times R \times T \times Md}$$

where, C is the headspace CH_4 concentration in ppm after 24 hours of incubation, HS is the volume of the headspace in cubic meters, P is the pressure in Pascals (101,325 Pa), μ

is the molar mass of CH_4 (=16 g/mol), R is the ideal gas law constant (8.3145 J/mol K), T is the temperature in Kelvins (294.15 K=21 °C), and Md is the dry weight of the soil sample in grams.

2.1.6 Soil Methanotrophy

To verify that methanotrophic oxidation follows first order reaction rate kinetics and can be approximated using an exponential decay function, four soil samples from the honohono meadow were incubated under high CH_4 concentrations and time-series measurements were made. To do so, the samples were placed in 150 mL serum bottles and sealed as described above. 12 to 50 ppm CH_4 was added to the headspace of each and the bottles were incubated at room temperature for 24 hours. One of them had a headspace methane concentration in the high affinity oxidation range described by Le Mer and Roger (2001), while the three remaining had CH_4 headspace concentration in the mixed affinity oxidation range (i.e., both low and high affinity oxidation ranges). Gas samples were then retrieved from each bottle and analyzed using the GC at regular intervals (2 to 3 hours) until 16 hours of incubation and then after 24 hours. Moreover, one bottle was filled with soil, autoclaved for 3 hours at 121 °C and incubated under high CH_4 levels (45 ppm) as a negative control. After the experiment, the soil was poured out of the bottles and dried as described in the previous section. The headspace methane content of each bottle was then plotted as a function of the sampling time (i.e., t=0, t=3 hrs…until t=24 hours). If methanotrophy follows first order reaction kinetics, the resulting curve can be fit with an exponential function:

$$C(t)=C_0e^{-kt}$$

where, C(t) is the CH_4 headspace concentration at time t in ppmv, C_0 is the initial CH_4 headspace content in ppm, k is the first order rate constant (hr^{-1}) and t is the time in hours. Fig. 6 shows the expected exponential decrease that resulted from the incubation of 4 soil samples from the honohono meadow under different CH_4 concentrations. The methane concentration in the autoclaved bottle remained constant over 24 hours indicating that the decreasing CH_4 levels observed in all the other incubation bottles are the result of CH_4 oxidation by methanotrophic bacteria rather than non biological processes. The fits of the high and mixed affinity oxidation experiments are shown on Fig. 7 and 8 respectively. Both high and mixed affinity oxidations are well fitted with an exponential decay function. Therefore, the assumption that methane oxidation follows first order reaction kinetics is verified.

Each methane oxidation rate constant given from fitting the exponential function was normalized by the mass of the dry soil:

$$K_{Normalized} = \frac{k}{M_{Dry\,Soil}}$$

Soil samples from the sedge meadow, honohono meadow, strawberry guava canopy, `ohi`a scrub and ti thicket were collected from the surface layer (0-20 cm) after each static chamber experiment and incubated under high CH_4 concentrations for 24 hours. The procedure used for these samples was identical except measurements were made at t=0 and t=24 hours. After 24-hours of incubation, the final methane concentration in each bottle had considerably decreased compared to initial levels and was close to atmospheric levels (i.e., 1.75ppmv). Moreover, the headspace CH_4

concentration of each autoclaved bottle remained constant after a 24-hour incubation time under high CH_4 levels.

The methane oxidation rate constants were calculated according to the following equation:

$$k = \frac{1}{24} \times \ln\left(\frac{C_0}{C_{24}}\right)$$

where, k is the rate constant in hr^{-1}, C_0 is the initial concentration of CH_4 in the headspace and C_{24} is the concentration of CH_4 in the headspace after 24 hours of incubation. The rate constant was then normalized using the dry mass of soil of each sample as discussed previously.

2.1.7 Root Tissue Methanotrophy

Another type of experiment was performed in order to estimate the rhizospheric methanotrophic activity in the honohono and sedge meadows. Root tissues from the species *Scirpus Validus* (Honohono Meadow) and *Cladium Leptostachyum* (Sedge Meadow) were incubated in 15 mL of tap water contained in 25 mL serum bottles sealed with butyl rubber stoppers and aluminum crimp seals. The root tissues were rinsed with tap water before adding them in the bottles, to remove the soil particles attached to the tissues. In each bottle, 15 mL of 100 ppm methane standard was injected. In the negative control bottle, no root tissue was added but just tap water and CH_4 (Heilman and Carlton, 2001). Changes in total CH_4 in the bottle's headspace were monitored every hours for six hours and then after 24 hours using the GC. The results of this experiment are not interpreted here but are shown in the Appendix.

2.2 Environmental Parameters

2.2.1 Precipitation

Ka`au crater rainfall has been measured since February 2003 using an ONSET RG2M rain gauge equipped with a tipping-bucket collector and a HOBO event data logger. One tip of the bucket occurs for each 0.2 mm of rainfall and the event data logger records the time of each tip. The rain gauge location in the crater is shown on Fig. 5. The rainfall record of the Palolo Valley station # 718 (NCDC NOAA, 2003) was correlated with the precipitation data recorded in the crater in order to approximate rainfall in Ka`au crater for periods when no data is available in the crater. From day 152 to 184 in 2003, the rain gauge was deployed next to the one in Palolo Valley to estimate the instrumental difference between the two gauges. The precipitation data from both rain gauges was averaged daily to calculate the correlation and instrumental difference. All data presented are daily averages.

2.2.2 Water Table Level

The water table level (WTL) was measured at two different locations in the crater using miniTROLL water level sensors. Each sensor was inserted into a 1.5 m PVC pipe into which holes had been drilled at regular intervals from top to bottom and introduced into the sediment. To correlate the WTL with net methane fluxes, one sensor was deployed in the honohono meadow next to the fixed static chamber from days 248 to 306. The second sensor was installed next to the rain gauge, 30 meters away from the other sensor to compare the WTL at two different locations. Before retrieving the sensors from the crater on day 306, the distance from the sensor to the sediment surface was measured. The sensor was 1.22 meters below the surface in the honohono meadow while the other

one was 1.27 meters below the surface next to the rain gauge. Each sensor was set to take a water table level and water temperature measurement every 15 minutes. Both data sets (i.e., from the honohono meadow and rain gauge location) were averaged daily.

2.2.3 Temperature

Temperature was recorded for the whole experimental period (i.e., day 242 to 306) using a Veriteq Spectrum 2000 data logger. Temperature data was also obtained from February to April 2003 using the same instrument. The logger was set to take a temperature measurement every 5 minutes. The data was then averaged for each day and correlated with net methane emissions.

2.2.4 Photosynthetically Active Radiation (PAR)

The PAR was recorded using a HOBO Micro Station equipped with an ONSET PAR smart sensor. A PAR measurement was taken every 5 minutes and stored in the micro station. All the PAR data presented in this paper are daily averages.

2.2.5 Soil Chemical Analysis

Soil samples from the Strawberry Guava canopy and sedge and honohono meadows were sent to the University of Hawaii College of Tropical Agriculture and Human Resources (CTAHR) Agricultural Diagnostic Center for Organic Carbon (OC), nitrogen and sulfur analysis. The OC and nitrogen content data presented in this paper are means of 3 replicates for the strawberry guava canopy and honohono meadow and means of 9 replicates for the sedge meadow. The standard deviation was calculated from the replicates. Only one sample per vegetation pattern was analyzed for sulfur content.

Figure 4. Static Chamber. Left: Static chamber collar with fan, Right: Gas sampling in the honohono meadow

Table 1. Static chamber sampling schedule. Seven incubations were performed in the honohono meadow, 3 in the sedge meadow and strawberry guava canopy and one in the `ohi`a scrub and ti thicket

Experiment Number	Day in 2003	Vegetation Pattern Chamber 1	Vegetation Pattern Chamber 2
1	242	Strawberry Guava	----------
2	250	Strawberry Guava	----------
3	264	Honohono meadow	Sedge meadow
4	271	Honohono meadow	Ohia scrub
5	278	Honohono meadow	Ti Thicket
6	285	Honohono meadow	Sedge Meadow
7	291	Honohono meadow	Honohono meadow
8	298	Honohono meadow	Strawberry Guava
9	306	Honohono meadow	Sedge meadow

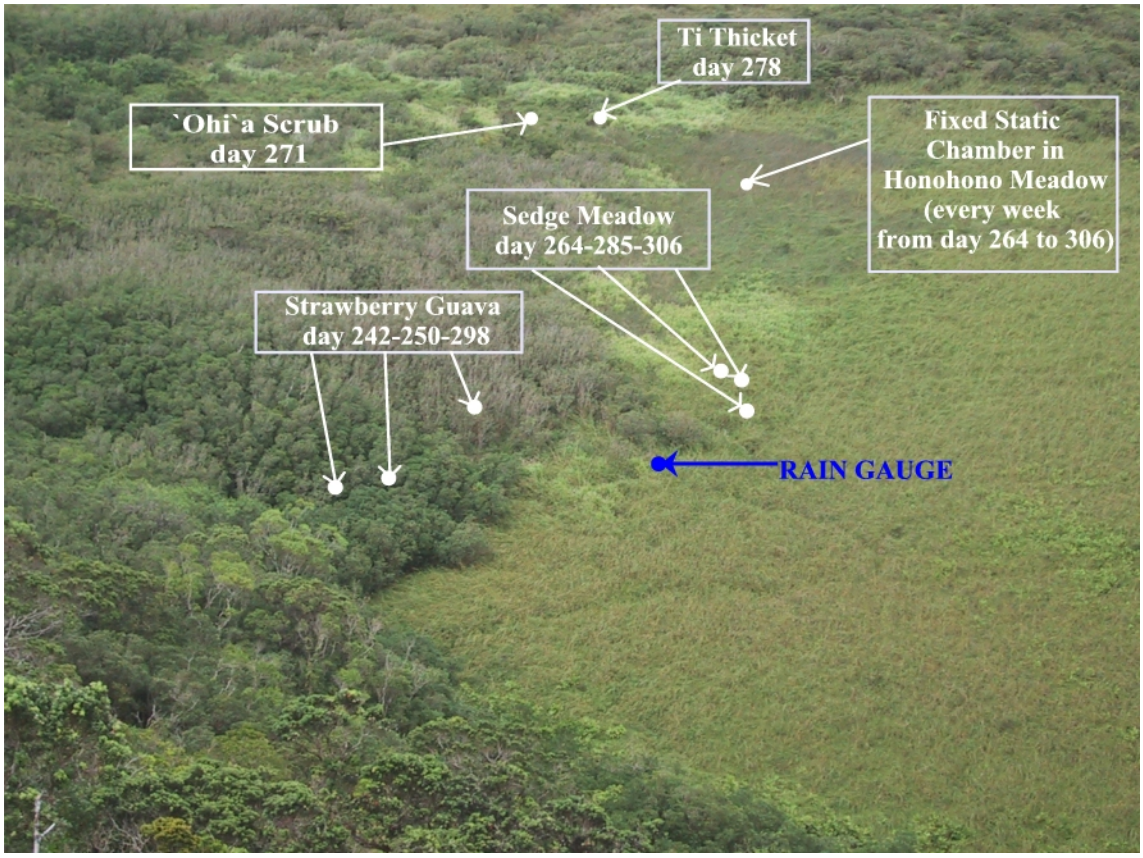

Figure 5. Static chamber sampling locations
All the dots represent a sampling location.

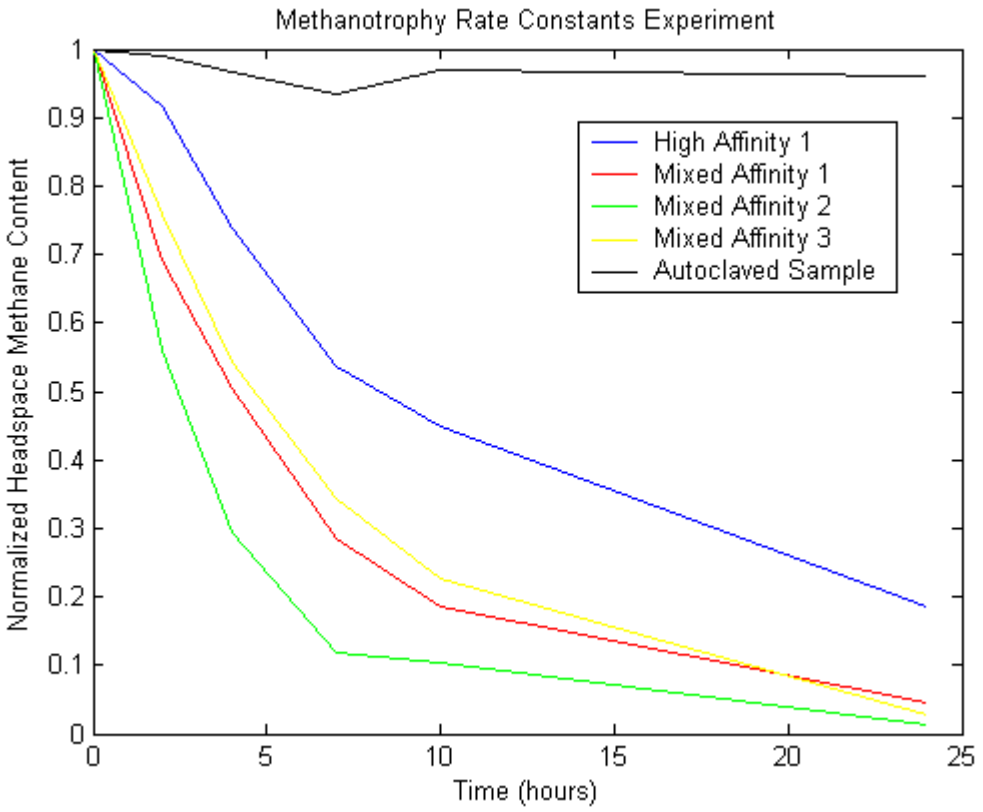

Figure 6. Methanotrophic oxidation over 24 hours.
High affinity 1: CH_4 initial= 11 ppm
High Affinity 2: CH_4 initial= 20 ppm
Low Affinity 1 CH_4initial=35 ppm
Low Affinity 2: CH_4 initial= 50 ppm
The autoclaved negative control (black line) headspace methane content remained constant over time

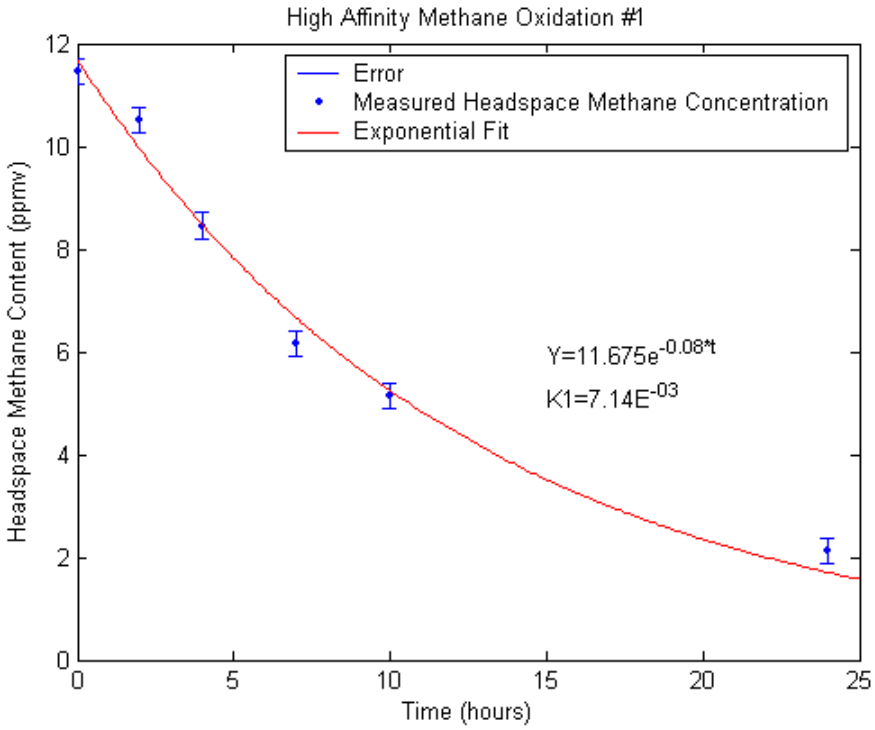

Figure 7. High affinity methane oxidation

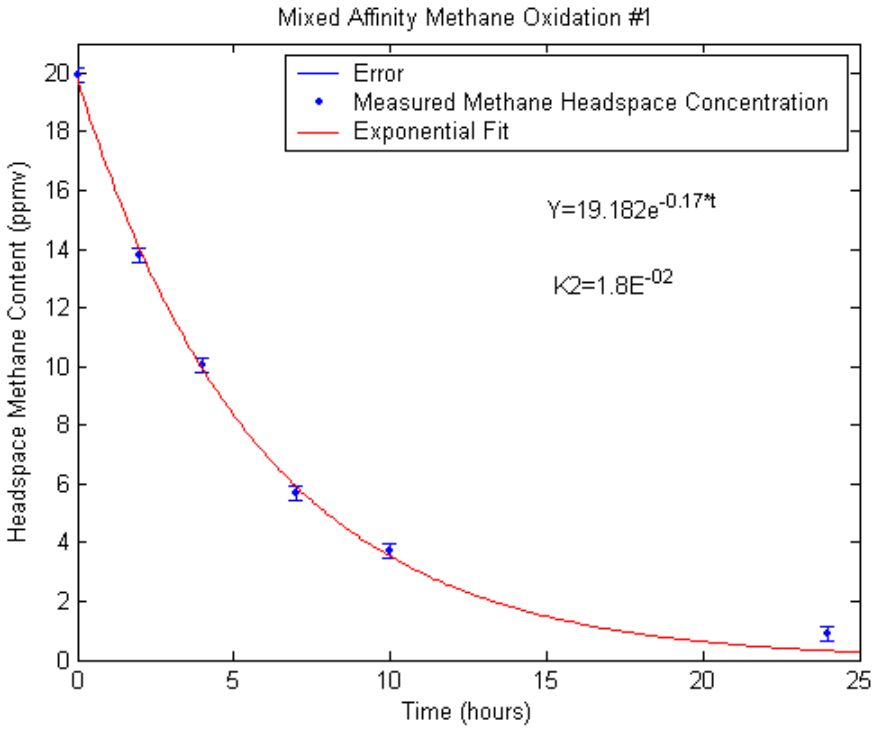

Figure 8. Mixed Affinity Methane Oxidation #1

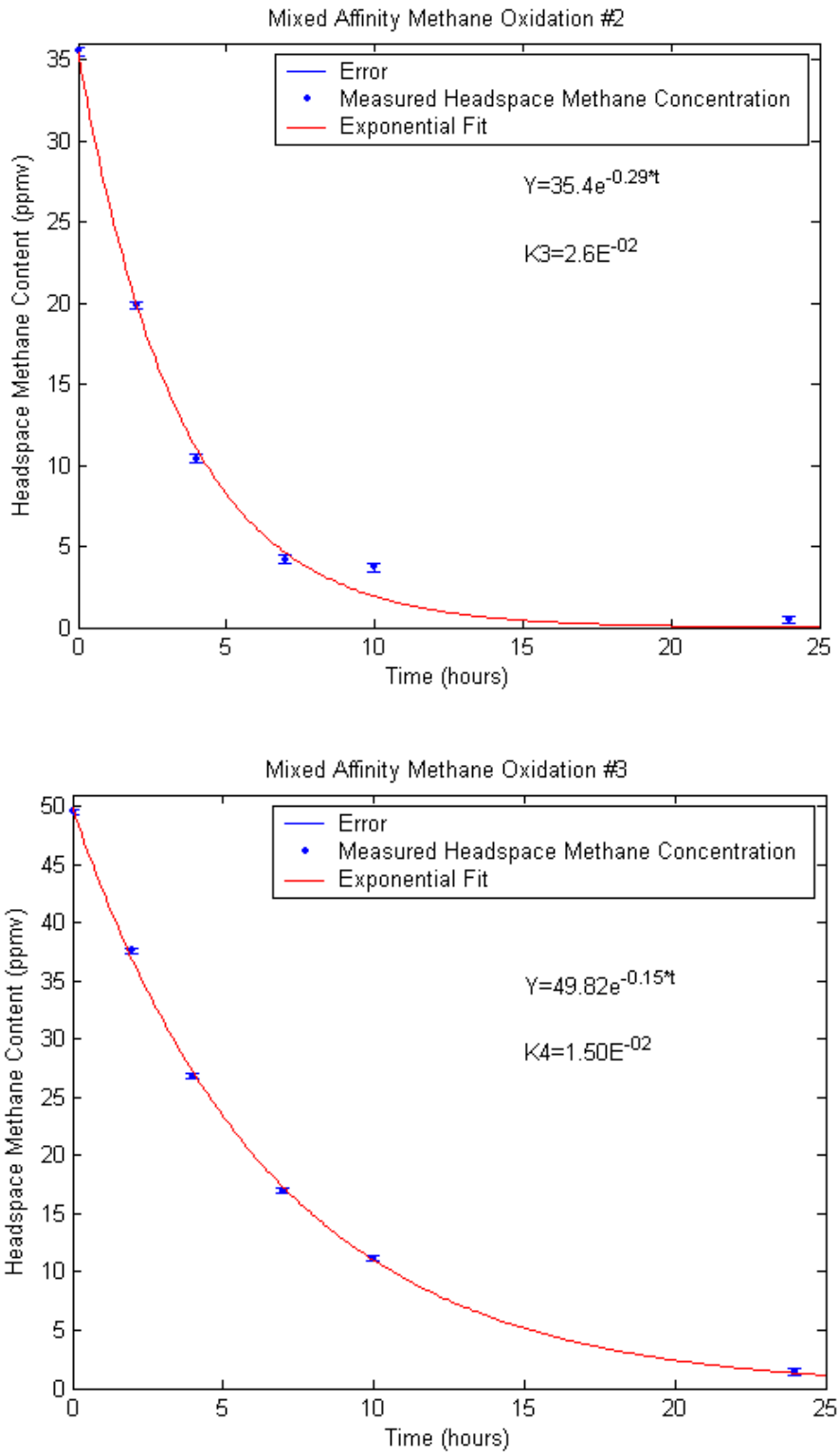

Figure 8. (continued) Mixed affinity methane oxidations # 2 & 3

3. RESULTS

3.1 Methane

3.1.1 Net Methane Flux

All results are shown on Table 2 and Fig. 9. The largest net methane flux was recorded in the ti thicket on day 278 (159 mg m^{-2} day^{-1}) and the lowest in the strawberry guava canopy on day 242 (1 mg m^{-2} day^{-1}).

3.1.2 Net CH_4 Flux Statistics

On day 291, both chambers were deployed next to each other in the honohono meadow in order to calculate the average and standard deviation of the net methane fluxes obtained (N=4 Table 3). Because the same experiment could not be performed in every vegetation pattern, it is assumed that the standard deviation of the measurements in the other vegetation patterns is approximately equal to the σ calculated using both chambers in the honohono meadow. The variance was calculated according to the following equation:

$$\sigma_{1+2}=(\sigma_1^2+\sigma_2^2)^{1/2}=16.56$$

For each static chamber incubation where the chambers were used simultaneously in two different vegetation patterns, the significance of a difference in flux Δ is:

$$\Delta = \frac{\left|F_1 - F_2\right|}{\sigma_{1-2}}$$

where, F_1& F_2 are the net CH_4 fluxes for vegetation patterns 1&2 and σ_{1+2} is the variance calculated above. Table 4 shows that, for all the incubations where the chambers were

used simultaneously in different vegetation patterns, the net methane flux difference is significantly larger than the uncertainty. The simultaneous use of the two chambers indicates that net methane emissions differ significantly between vegetation patterns under similar climatic conditions (i.e., temperature, PAR and precipitation but not necessarily water table level). This suggests that, plant communities may influence the net CH_4 emissions from the Ka`au crater wetland

3.1.3 Methane Generation Potential

Table 5 and Fig.10 summarize the surface net methane generation potential measured in the different plant communities. All CH_4 production potential have units of $mg(CH_4)\ g(dry\ soil)^{-1}\ day^{-1}$. The largest CH_4 generation potential rate was measured in the `ohi`a scrub on day 242 and the lowest was recorded in the strawberry guava canopy on day 298. In every vegetation pattern, the CH_4 production potential varies considerably from one sampling time to the other. For example, in the honohono meadow, the highest rate was recorded on day 291 ($1*10^{-3}$) and the lowest on day 278 ($4*10^{-5}$). The higher flux is thus 29 times larger than the lower flux.

3.1.4 Soil Methanotrophy

The normalized first order methane oxidation rate constants corresponding to the initial CH_4 headspace concentration injected in each bottle are shown in Table 6. This table suggests that mixed affinity oxidation may have a larger rate constant compared to high affinity oxidation. High affinity oxidation has a rate constant of 0.007 hr^{-1} $g(dry\ soil)^{-1}$ and the average mixed oxidation rate constant is 0.019 $hr^{-1}g(dry\ soil)^{-1}$. Initial CH_4 headspace concentrations increasing from 11 to 35 ppm lead to increasing rate constants

(0.07 to 0.026 hr^{-1} g(dry soil)$^{-1}$). However, the methane oxidation rate constant was lower than the two other mixed affinity oxidations with a CH_4 concentration of 49 ppmv (k=0.015 hr^{-1} g(dry soil)$^{-1}$). Moreover, as low and high affinity oxidations have different rate constants it would be more accurate to fit both affinities with two different exponential functions.

The methane oxidation rate constants from surface soil samples collected after each static chamber incubation are shown in Table 7. The highest oxidation rate constant was recorded in sediment collected from the honohono meadow on day 306 (0.026 hr^{-1}g(dry soil)$^{-1}$). The lowest rate constants were recorded in the `ohi`a scrub and honohono meadow (0.008 hr^{-1}g(dry soil)$^{-1}$) on day 242 and day 264 respectively. The oxidation rate constants averaged 0.014 ± 0.006 hr^{-1} g(dry soil)$^{-1}$ in the honohono meadow (N=7) and 0.011 ± 0.002 hr^{-1} g(dry soil)$^{-1}$ in the sedge meadow (N=3).

3.2 Environmental Parameters

3.2.1 Precipitation

Using the Ka`au crater-Palolo Valley rainfall correlation and the instrumental difference, the Ka`au crater rainfall was approximated from November 2002 to November 2003 and approximated over a year. Rainfall data from Ka`au crater and Palolo Valley were correlated over two different periods; February to May and August to October 2003. A strong correlation was found between the two sites ($R^2$=0.94 from February to May and $R^2$=0.97 from August to October. Fig.11 & 12). The Ka`au crater rainfall (Fig. 13) from November 2002 to November 2003 can be approximated using the Palolo Valley rainfall according to the following relation:

$$\text{Ka`au Crater Precipitation} = 1.25 \times \text{Palolo Valley Precipitation}$$

where, 1.25 is the average of the slopes of the two fits shown in Fig. 11 and 12.
Ka`au crater receives more rainfall, presumably due to its proximity to the Ko`olau crest and a stronger orographic effect. The deployment of the rain gauge next to the Palolo Valley one to estimate the instrumental difference between the two gauges was unsuccessful. The data downloaded from the rain gauge were incoherent with the Palolo Valley data. It was expected that the data retrieved from the respective rain gauges would be equal or that one rain gauge would record a slightly larger or smaller amount of rainfall compared to the other. Yet, no consistent pattern was observed between the data. For example, on June 17 the Palolo Valley rain gauge recorded 0.75 mm of rain while the 12 mm was recorded by our rain gauge. Three days later the Palolo Valley gauge recorded 8.5 mm of rain while the other recorded 0.6 mm. This contradiction prevented

any comparison of both data sets and the instrumental difference between the rain gauges could not be approximated and was not included in the equation depicted above. The rain data from Ka`au crater was lost once due to instrumental failure. The Ka`au crater-Palolo Valley correlation was used to "patch" the gaps in the Ka`au crater rainfall dataset (Fig. 11 and 12). Unfortunately, both rain gauges were out of service for two weeks in July and no rain data is available for this period. The total rainfall in Ka`au crater amounts to 2656 mm from November 2002 to November 2003 excluding day 250 to 263 when both rain gauges were out of service. The wettest period was recorded from November to late April and the driest from late April to early September.

3.2.2 Water Table Level (WTL)

The honohono meadow WTL is presented in Fig. 14. The WTL is strongly correlated (R^2=0.97) between the two sites indicating that precipitation, surface drainage and eventually groundwater drainage fluxes are similar at the two locations (Fig. 15). However, the WTL at the rain gauge station was 0.15 m higher than in the honohono meadow (Fig. 15). The WTL was the highest for the static chamber incubations performed on day 285 and 291, the lowest for the incubations completed on day 242 and 278 and at an intermediate level on day 298 and 306. The distance from the sensor to the soil surface suggests that the water table never reached the surface in the honohono meadow (Fig.14). On the field, however, it appeared that the WTL was above the soil surface on several occasions. It is possible that the sensor was not inserted perpendicularly in the soil. In this case, the distance measured from the sensor to the surface would be longer than the reality, which explains why Fig. 14 indicates that the

WTL never reached the surface. It is also possible that the drainage was poor from the surface into the soil at this location.

3.2.3 Temperature

The daily air temperature of Ka`au crater from February to August is presented on Fig. 16. Several months of data are missing because the data logger had to be retrieved to the lab to download the data and was brought back to the crater a few weeks later. Also, some data sets were lost by instrumental malfunction. The mean temperature for the periods in which data were recovered was 21.5 ± 1.90 °C from February to November 2003. From February to April, the average temperature was 19.84 ± 1.65 °C and it was 22.59 ± 0.74 °C from July to November. Therefore, Ka`au crater experiences a weak temperature seasonality throughout summer and winter months. This agrees with the mean 22 ± 2-3 °C average temperature reported by Armstrong (1983).

3.2.4 Soil Chemical Composition

The total organic carbon, nitrogen and sulfur content of the honohono meadow, sedge meadow and strawberry guava soils are shown on Table 8 and Fig. 17. Organic carbon and nitrogen content were similar in the honohono and sedge meadows and strawberry guava canopy. However, sulfur content differed considerably from one community to the other with 53µg g(dry soil)$^{-1}$ for strawberry guava soils, 110µg g(dry soil)$^{-1}$ for sedge meadow soils and 81µg g(dry soil)$^{-1}$ for the honohono meadow soil. The uncertainty of these measurements is not know as only 1 sulfur measurement per vegetation pattern was performed.

3.2.5 Photosynthetically Active Radiation (PAR)

Table 9 and Fig.18 show that there is no significant correlation between net CH_4 fluxes from the honohono meadow and PAR (R^2=0.081). All PAR data are given in units of microeinsteins (μE). The daily average PAR throughout the experimental period is plotted in Appendix II

Table 2. Net methane flux from 5 vegetation patterns
Units are in mg (CH_4) m^{-2} day^{-1}

Day in 2003	Honohono Meadow	Sedge Meadow	Strawberry Guava Canopy	`Ohi`a Scrub	Ti Thicket
242	----	----	1	----	----
250	----	----	77	----	----
264	68	8	----	----	----
271	78	----	----	135	----
278	57	----	----	----	159
285	52	25	----	----	----
291	89	----	----	----	----
298	146	----	12	----	----
306	94	18	----	----	----
Average	**83**	**17**	**30**	**135**	**159**
Std Dev (σ)	**31**	**8**	**41**	**0**	**0**
Standard Error of Mean	**12**	**5**	**24**	**0**	**0**

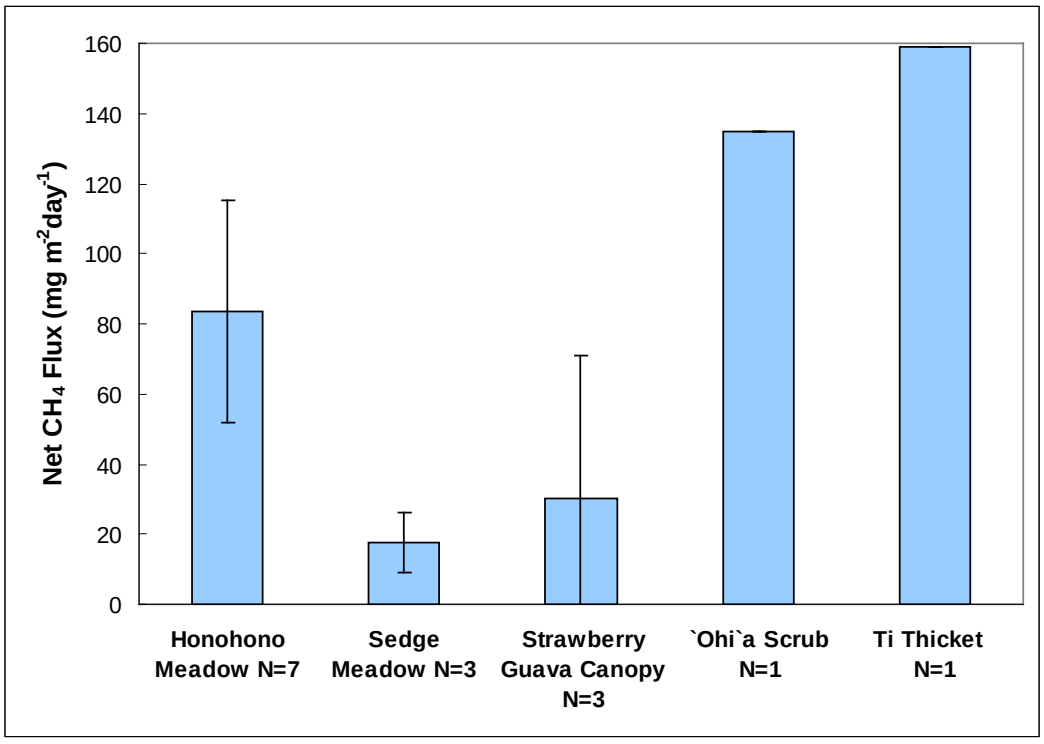

Figure 9. Net methane emissions in 5 vegetation patterns
Units: mg (CH_4).m^{-2}.day^{-1}. Error bars are the standard deviation.

Table 3. Net CH_4 emission in the honohono meadow using both chambers
Units: $mg(CH_4)\ m^{-2}\ day^{-1}$

Chamber 1	Chamber 2
78	90
105	82
Overall Average	91
Std Dev. (σ)	12

Table 4. Calculation of Δ

Vegetation Pattern Compared	Δ
Honohono - Sedge	3.6
Honohono - Sedge	1.6
Honohono - Sedge	4.6
Honohono - S. Guava	8.1
Honohono - `Ohi`a	3.4
Honohono - Ti	6.2

Table 5. Surface soil CH_4 generation potential
Units: mg(CH_4) g(dry soil)$^{-1}$day^{-1}

Date	Honohono Meadow	Sedge Meadow	Strawberry Guava	`Ohi`a Scrub	Ti Thicket
242	----	----	$1.3*10^{-5}$	----	----
264	$1.44*10^{-4}$	$6*10^{-5}$	----	----	----
271	$6*10^{-5}$	----	----	$1.35*10^{-3}$	----
278	$4.3*10^{-5}$	----	----	----	$2.75*10^{-4}$
285	$3.64*10^{-4}$	$1.2*10^{-5}$	----	----	----
291	$1.253*10^{-3}$	----	----	----	----
298	$2.23*10^{-4}$	----	$6*10^{-6}$	----	----
306	$1.03*10^{-4}$	$8*10^{-6}$	----	----	----
Average	$3.12*10^{-4}$	$2.6*10^{-5}$	$9*10^{-6}$	$1.35*10^{-3}$	$2.75*10^{-4}$

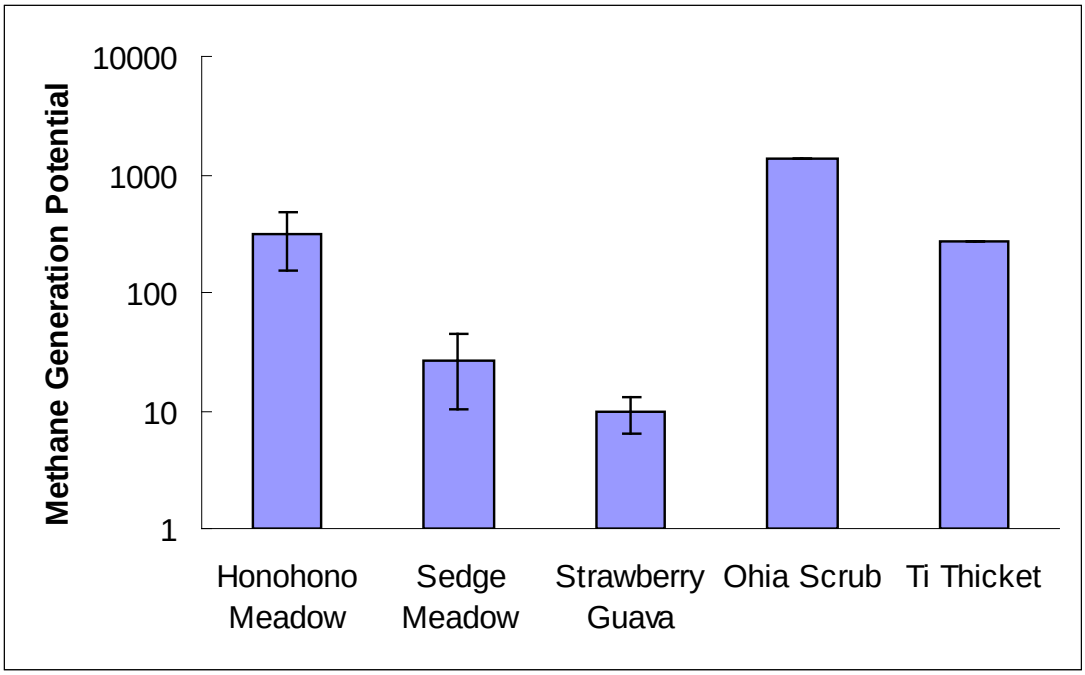

Figure 10. Average methane generation potential in 5 vegetation patterns
Units: mg(CH_4) g(dry soil) day^{-1}. Error bars are the standard deviation.
Only single measurement was obtained in the `ohi`a scrub and ti thicket.
The y-axis is a log scale

Table 6. Methane oxidation rate constants from fits
K1: From fit in Fig. 7 , K2,K3&K4: From fit in Fig. 8
Units: hr^{-1} $g(dry\ soil)^{-1}$

Initial Methane Headspace Content (ppm)	Oxidation Rate Constant
11.39	K1=0.007
19.79	K2=0.018
35.28	K3=0.026
49.34	K4=0.015

Table 7. Methanotrophic oxidation rate constants in the 5 vegetation patterns studied
Units: hr^{-1} $g(dry\ soil)^{-1}$

Days in 2003	Honohono Meadow	Sedge Meadow	Strawberry Guava	`Ohi`a Scrub	Ti Thicket
242	----	----	----	----	----
264	0.008	0.010	----	----	----
271	0.012	----	----	0.008	----
278	0.009	----	----	----	0.011
285	0.013	0.014	----	----	----
291	0.014	----	----	----	----
298	0.016	----	0.011	----	----
306	0.026	0.009	----	----	----
Average	0.014	0.011	0.011	0.008	0.011

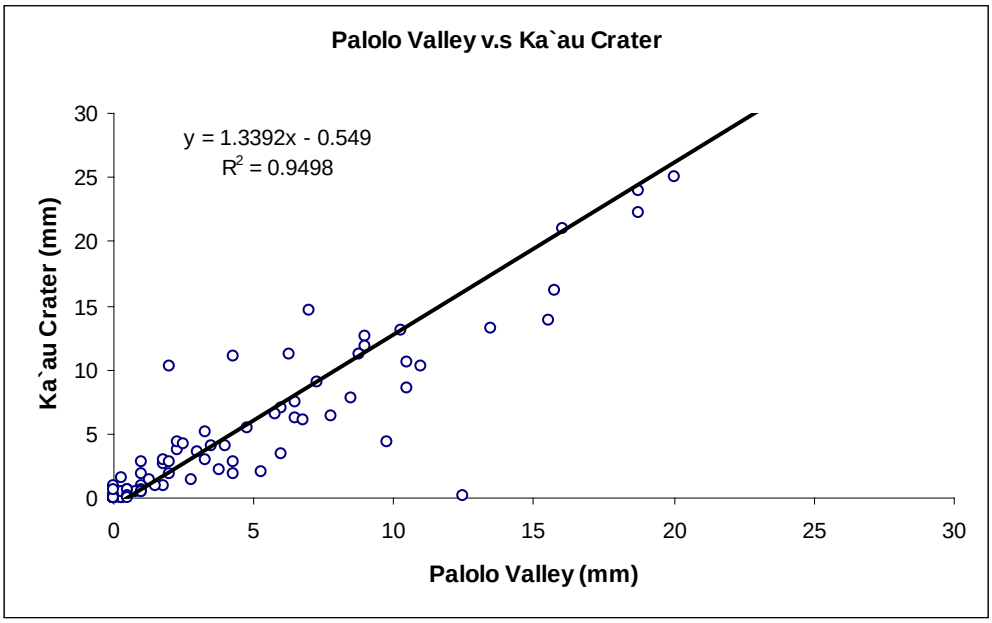

Figure 11. Palolo Valley Ka`au Crater correlation February to May 2003

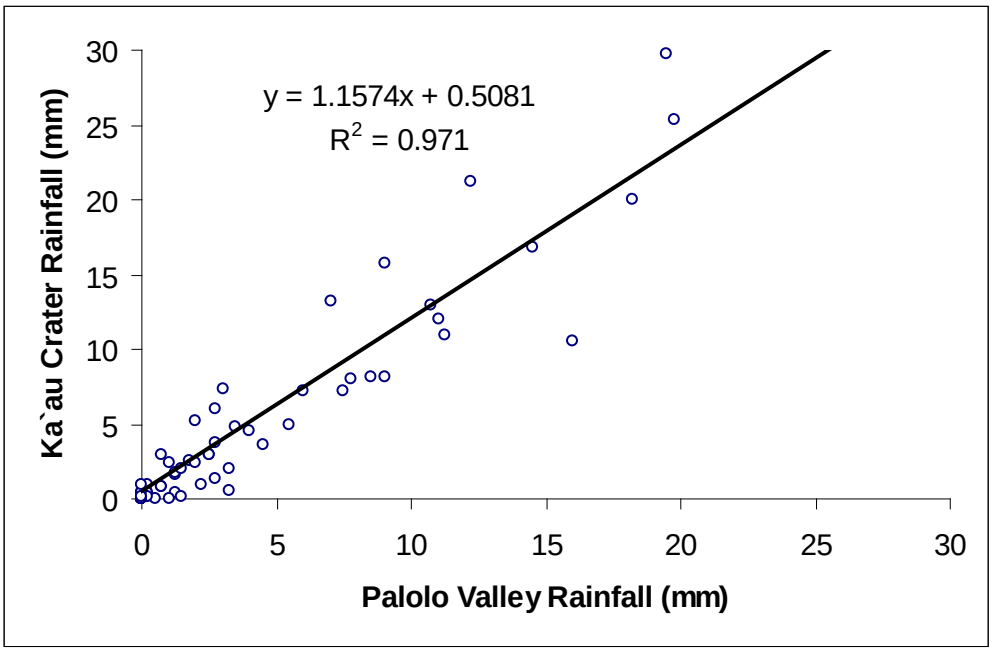

Figure 12. Palolo Valley-Ka`au Crater rainfall correlation August to November 2003

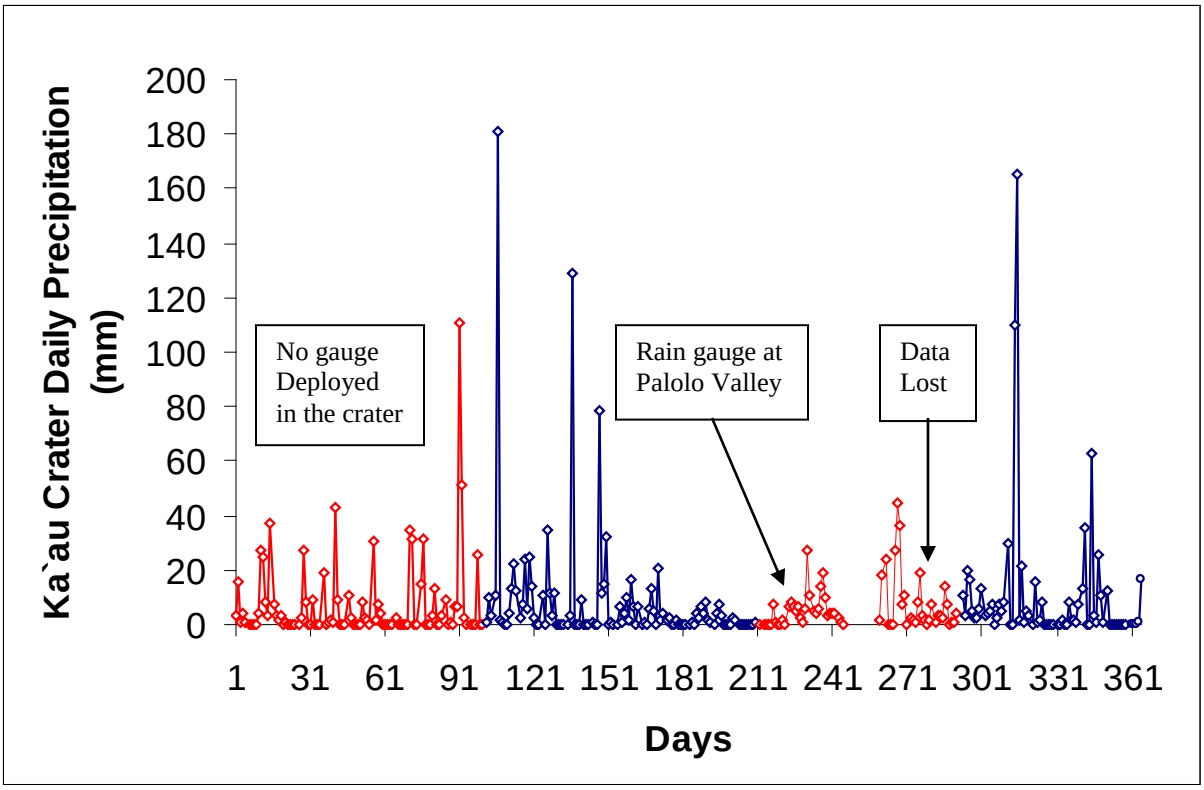

Figure 13. Ka`au Crater rainfall November 2002 to November 2003
In red: Rain data approximated using the Palolo Valley rainfall record and the rainfall correlation. There is a "data gap" from day 250 to 263 when both rain gauges (Palolo and Ka`au crater) were out of service.

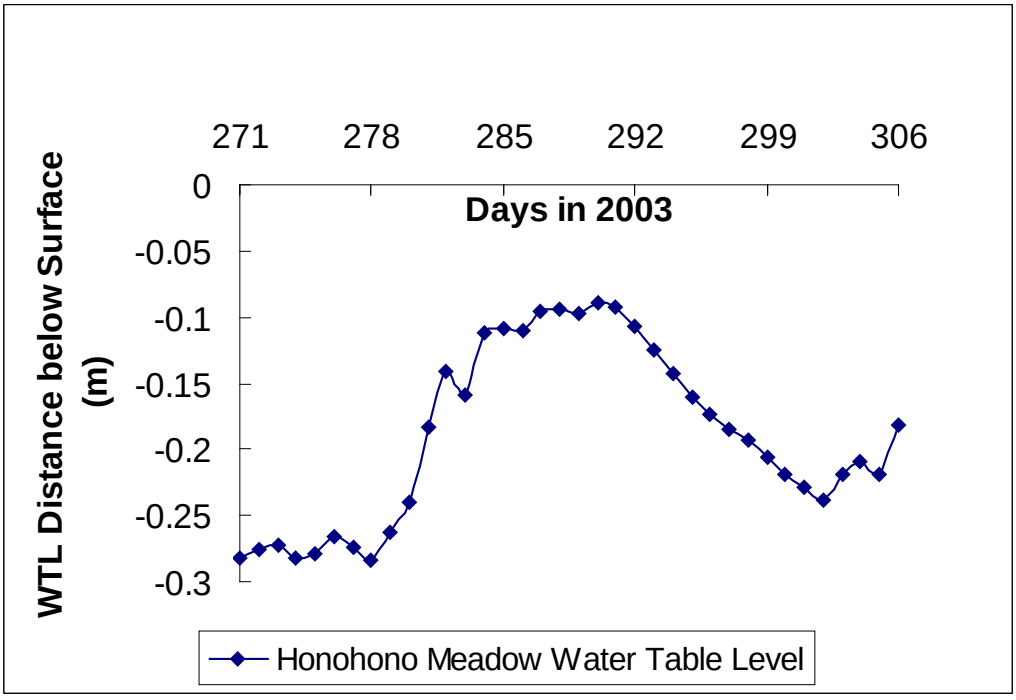

Figure 14. Honohono meadow WTL distance below the surface throughout the sampling period

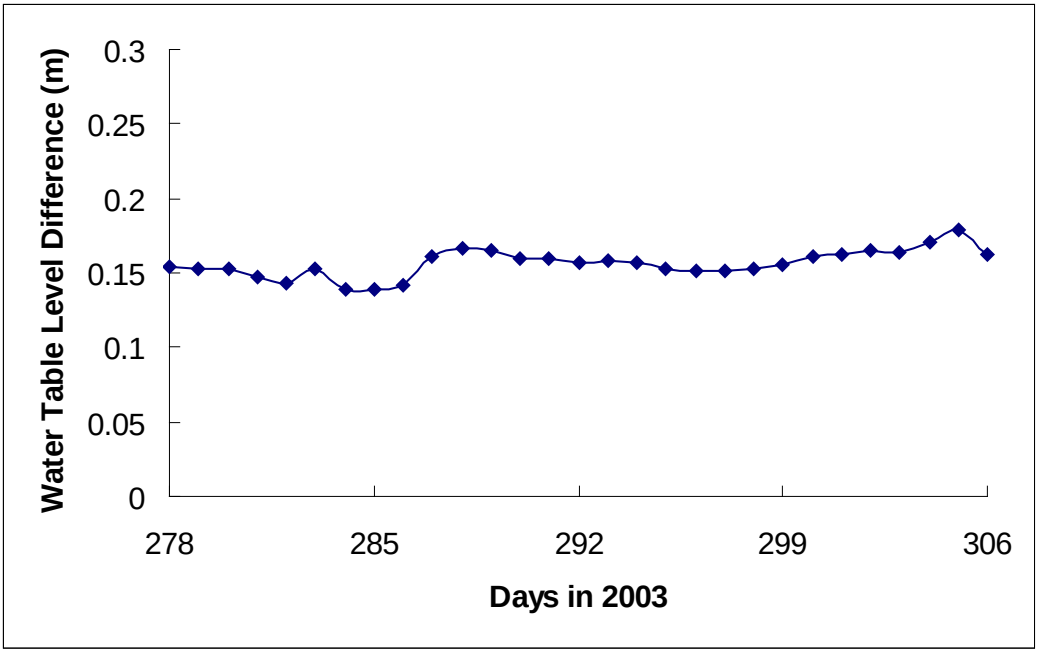

Figure 15. Rain gauge site-Honohono WTL difference
The mean WTL in the honohono meadow is 0.15 meters lower than at the rain gauge site. This blue line suggests that the WTL at both monitoring sites varies in the same manner.

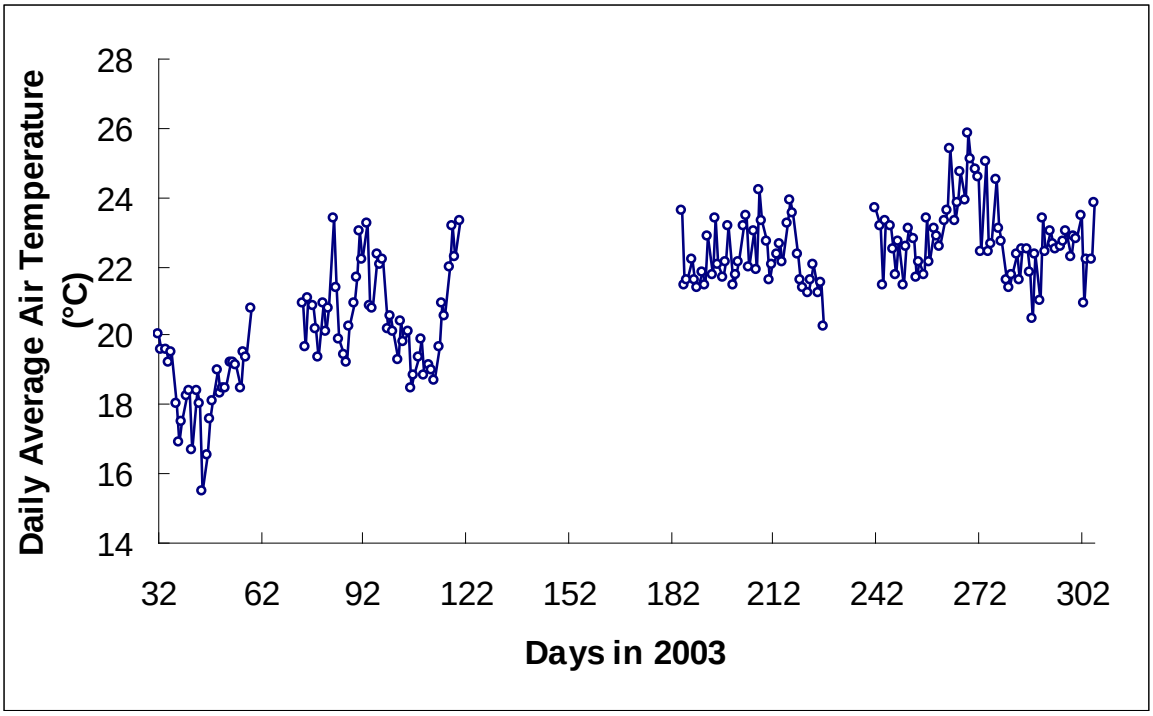

Figure 16. Ka`au Crater temperature from February to November 2003

Table 8. Soil Chemical Composition
Units: % dry weight of soil. Errors are the standard deviation between replicate samples.

	Strawberry Guava	Sedge Meadow	Honohono Meadow
Organic Carbon (%dry weight)	41 ± 5	34 ± 6	35 ± 3
Nitrogen (%dry weight)	2.1 .± 0.2	2.5 ± 0.5	3.0 ± 0.3
Sulfur (µg g(dry soil)$^{-1}$)	53	110	81

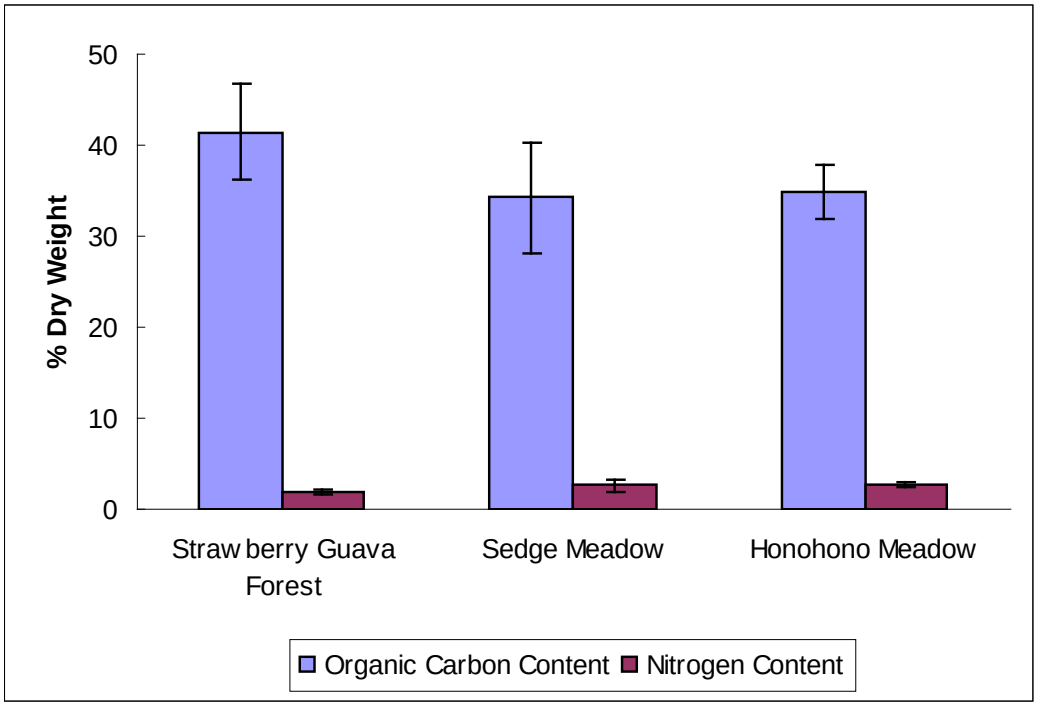

Figure 17. Soil Chemical Composition
Error Bars are the standard deviation

Table 9. PAR and net methane flux recorded in the honohono meadow
Net CH_4 Flux in mg m^{-2} day^{-1} and PAR in µE

Date	Net Methane Flux in Honohono Meadow	PAR (µE)
264	69	396
271	78	413
278	57	403
285	52	103
291	89	149
298	146	184
306	94	252

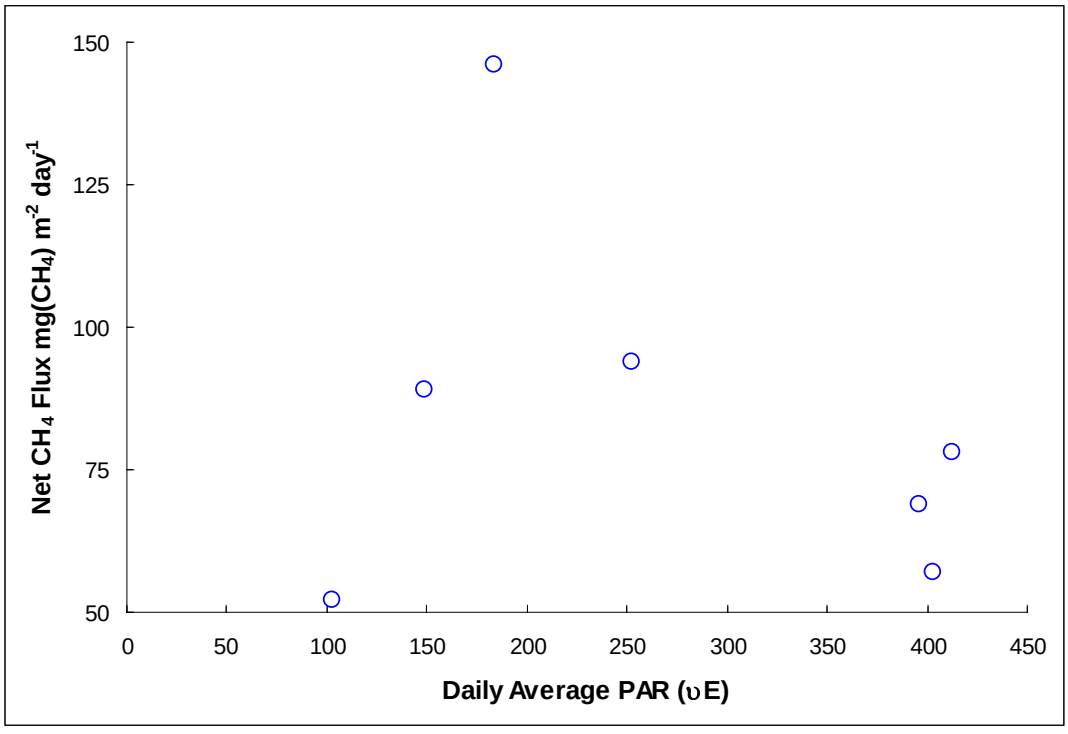

Figure 18. PAR-Honohono meadow net CH_4 emission comparison

4.) DISCUSSION

4.1 Methane

4.1.1 Average Net Methane Fluxes

There was an accumulation of methane in the chambers to varying amounts in every vegetation pattern after a 2-hour incubation time. The first main conclusion that can be drawn is that the Ka`au crater wetland is a net source of methane to the atmosphere.

The largest net CH_4 flux variations within a single plant community was recorded in the strawberry guava forest (σ= 41 mg(CH_4) m^{-2} day^{-1}, Table 2). This is probably because the WTL varied considerably among the three different static chamber sites. Several small depressions are found in the strawberry guava forest where the water table reaches the surface, forming small ponds. On day 250, the 2-hour static chamber incubation was performed in a waterlogged soil next to one of these ponds. A high water level increases the width of the reduced soil layer hosting methanogens and reduces the width of the oxidized zone hosting methanotrophs. Therefore, more CH_4 is produced than oxidized which explains the high net CH_4 flux measured on day 250. Large net CH_4 emission variations were also recorded in the honohono meadow (σ =31 mg(CH_4) m^{-2} day^{-1}). In this vegetation pattern, 7 incubations were performed at the exact same place throughout the entire period. Therefore, the differences recorded at this site reflect fluctuations in environmental parameters (such as precipitation and water table level) rather than site-specific variations.

In the honohono meadow, the largest net methane flux was ~3 times larger than the smallest one (comparison of CH_4 flux from day 298 and day 285, Table 2). It is possible that methane fluxes in all other vegetation patterns may also vary by a factor of

3. Only one incubation was performed in the ti thicket at a time where the honohono meadow CH_4 flux was low (=57 mg m^{-2} day^{-1}). This suggests that the ti thicket flux recorded on day 278 may not also be low. If the ti thicket CH_4 flux was measured on day 298, at a time where the honohono meadow flux was the largest, a larger flux may have been recorded in this pattern. The same logic can be used for the `ohi`a scrub.

The average net methane flux from 5 different vegetation patterns weighted by their 1969 areas over a 6 week period in Ka`au crater wetland was 84 ± 4 mg $m^{-2}$ $day^{-1}$. The global average methane flux from 1,600,000 km² of tropical wetlands (Matthews and Fung, 1987) was 50-137 mg $m^{-2}$ $day^{-1}$. The average net methane emission per square meter in Ka`au crater is thus within the range of the global emissions estimation from tropical wetlands. The average net methane emission rate in the crater is higher than the flux reported by Chang and Yang (2003) from the Kuan-du wetland in Thailand (43 mg m^{-2} day^{-1}). However, it is lower than the flux reported by Öquist and Svensson (2002) from a subarctic mire (156 mg m^{-2} day^{-1}).

The annual average net methane emission escaping the 200,000 m² Ka`au crater wetland from five different vegetation patterns over a 6 weeks experimental period is 5.8 ± 0.4 t($CH_4$) $yr^{-1}$. The `ohi`a scrub was the most important contributor to the overall methane emissions from the crater and the least was the strawberry guava canopy. The contribution of each vegetation pattern to the overall CH_4 emission escaping the wetland is shown in Table 8 and Fig. 19.

All the net methane flux measurements described above exhibit several limitations. First of all, the estimation of the areas of the 5 vegetation patterns in the Ka`au crater wetland was performed using a map made from a 1969 aerial photograph

from Kennedy (1975). Therefore, the daily average net CH_4 emission from Ka`au crater reflects the 1969 vegetation patterns areas. The crater vegetation has been changing over the last century with a shift from an `ohi`a wet forest to wetland-adapted species such as sedges and reeds (Kennedy, 1975). Today, the sedge meadow looks larger than the `ohi`a scrub. The average net methane flux from the `ohi`a scrub per square meter is roughly 4.5 times larger than the sedge meadow flux. If the actual size of the `ohi`a scrub and sedge meadow was taken into consideration, the overall net $CH_4$ emission escaping the Ka`au crater wetland is likely to be smaller than 5.8 ± 0.3 $t(CH_4).yr^{-1}$. Also, the contribution of the `ohi`a scrub to the overall methane flux escaping Ka`au crater is subject to large uncertainties as only one incubation was performed in this pattern.

Perhaps the major limitation of the static chamber experiments is that most measurements were performed with few or no plants in the chamber. In the honohono meadow, for the fixed chamber experiment, the same number of plants (*Scirpus Validus*) was inserted in the chamber for each incubation. However, it was not possible to insert plants in the chamber in the sedge meadow. Sedge meadow plants form dense root mats above the sediment, preventing the insertion of plants within the chamber at this location. Le Mer and Roger (2001) suggested that plants with an aerenchyma favor CH_4 emission by providing a natural conduit to transport CH_4 to the atmosphere. Larger CH_4 emissions can be expected in vegetated areas relative to non-vegetated sites. Consequently, the larger methane flux recorded in the honohono meadow may reflect plant mediated CH_4 transport compared to the sedge meadow flux.

Finally, the net methane flux measurements were confined in the southeastern most part of the crater (Fig. 5) and the locations of the chamber incubations were more

chosen on the basis of their accessibility rather than on a random basis. The IPCC (2001) reported that local emissions from most natural wetlands could vary considerably over a few meters. Hence, in order to improve the net methane emission estimates, a wider area of the crater should be studied.

4.1.2 Past and Future CH_4 Emission Scenarios

Several methane emission scenarios (Fig. 20) can be proposed based on the changes in the vegetation patterns observed in the Ka`au crater wetland since the early 1900s. In 1909, `ohi`a forest covered most of the crater (Kennedy, 1975). In the "1900 scenario", it is assumed that the `ohi`a scrub covered the entire crater (i.e., ~200,000 $m^2$) and that the net methane flux from the `ohi`a pattern at this time was similar to the flux recorded today. In this case, 9.5 $t(CH_4)\ yr^{-1}$ was released to the atmosphere at the beginning of the $19^{th}$ century. Since then, the `ohi`a scrub pattern decreased in size while the sedge meadow, honohono meadow, strawberry guava forest and ti thicket spread in the crater. In the "1969 scenario", the overall methane flux escaping Ka`au crater is $5.8 \pm 0.3\ t(CH_4)\ yr^{-1}$. As was mentioned previously, the contemporary CH_4 flux escaping the crater is likely to be smaller than in 1969. Therefore, net methane emissions from the Ka`au crater wetland may have significantly decreased over the last century as a result of vegetation changes. In the future, two vegetation changes scenarios are plausible. By comparing the 1975 vegetation maps from Kennedy (1975) with current photographs of the crater, it is clear that the sedge meadow and strawberry guava continue to spread while the `ohi`a scrub continue to recess. In addition, several strawberry guava patches that were not mentioned in Kennedy's work (1975) are now visible in the `ohi`a scrub.

Therefore, two extreme future scenarios are envisioned. In the first one, the sedge meadow colonizes the entire crater replacing every other pattern and in the second one, the strawberry guava takes over. Both scenarios suggest that the net methane emission from the Ka`au crater wetland would be much lower than today; $1 \pm 0.5$ t($CH_4$) $yr^{-1}$ for the sedge scenario and $2 \pm 3$ t($CH_4$) $yr^{-1}$ for the strawberry guava scenario. Hence, methane emissions from the Ka`au crater wetland are likely to have significantly declined since the early 1900s and this trend is expected to continue in the next decades if the sedge meadow and strawberry guava forest keep spreading.

4.1.3 Methane Generation and Oxidation Potentials

For every experiment in every vegetation pattern, varying amounts of methane were produced under anaerobic conditions during a 24-hour incubation time. This rate measurement presumably reflects the total activity of methanogenic Archea present at the soil surface at the time of sampling. It is assumed that the growth of the methanogen population in 24 hours is small. The higher the CH_4 generation potential of the soil, the more numerous the methanogens are and reciprocally. Moreover, the average net methane fluxes (Fig.9) and the average surface methane generation potentials (Fig.10) are approximately correlated between plant communtities. The highest average net CH_4 fluxes were recorded in the `ohi`a scrub and ti thicket, followed by the honohono meadow. The same pattern was observed for the surface CH_4 production potentials. Conversely, the lowest average net CH_4 fluxes were recorded in the strawberry guava and sedge meadow as were the lowest CH_4 generation potentials. Therefore, the variation in

net methane emissions are reflected in part by the variation in the activity of methanogens.

No oxidation rate constants data was found in the literature for tropical wetlands. Kettunen et al. (1999) reported methane oxidation potentials (first order rate constants) ranging between 0.010 and 0.129 $hr^{-1}g(dry\ soil)^{-1}$ in two Finnish mires. The minimum oxidation rate constant reported by the researchers is comparable to the minimum rate constants recorded in Ka`au crater for this study. However, the maximum oxidation potential recorded in the Finnish mire (0.129 $hr^{-1}g(dry\ soil)^{-1}$) is much larger than Ka`au crater (0.026 $hr^{-1}g(dry\ soil)^{-1}$). The oxidation rate constants measured in Ka`au Crater were thus in the same order of magnitude as other measurements.

4.2 Methane Fluxes and Environmental Parameters

4.2.1 Temperature

Fluctuations in CH_4 production over time may result from temperature variations. Le Mer and Roger (2001) reported that the Q_{10} for CH_4 generation equals 4.6 (increase of microbial activity after a 10 °C increase in temperature). Based on this number, it is possible to calculate the variations of methanogenic activity after a 1.90 °C increase in temperature according to the following equation:

$$R = \frac{f(T + \Delta T)}{f(T)} = e^{\frac{\Delta T \times \ln(Q_{10})}{10}}$$

where, R is the relative increase in activity after a temperature increase of 1.90°C, ΔT is 1.90°C and Q_{10} is 4.6. With a temperature variation of 1.90°C (which roughly corresponds to the seasonality in the air temperature of Ka`au crater for the whole experimental period) the methanogenic activity can increase by ± 33%.

However, it is important to remember that the ± 1.90 °C variation corresponds to air temperature. Methane production occurs at depth; in the anaerobic layers of the soil and temperature variations in the soil will be substantially smaller than air temperature variations. Air cools or warms faster than waterlogged soils because it takes more energy to warm air than water (=sensible heat) and because temperature conduction through soils is slow. Therefore, the relative increase in activity calculated above is probably larger than what actually happens in the soil. Each water level sensor was also recording the water temperature at both sites. In the honohono meadow, the water temperature averaged 20.82 ± 0.05 °C throughout the 6 weeks of soil sampling. Because the honohono soil is waterlogged at depth, the water temperature must equal the soil

temperature. Therefore, the increase in methanogenic activity related to the increase in soil temperature over time can be approximated using the equation described above. The variation in activity for a ± 0.05 °C temperature variation is estimated to be ± 0.7%. Each methane generation potential fluxes presented in Table 5 in the honohono meadow are at least 7% different from each other (this was calculated by using the data of day 278 and 285 on Table 5). Hence, the methane generation potential of the honohono meadow cannot be related to temperature fluctuations. In tropical wetlands such as Ka`au crater, where the seasonality is weak, temperature is not an important factor regulating methane emissions. This result agrees with the literature results (Le Mer and Roger, 2001; Miyajima et al., 1997). Other processes, such as precipitation, water table level, soil chemical composition and PAR must be the main parameters driving methane flux fluctuations over time.

4.2.2 Soil Chemical Composition and Photosynthetically Active Radiation

The organic carbon (OC) content of the honohono and sedge meadows and strawberry guava canopy is comparable. Therefore, the different net methane emissions recorded among these three vegetation patterns cannot be attributed to soil organic carbon content differences (Table 8 and Fig.17). Moreover, the soil OC content in Ka`au crater is extremely high (~40% dry weight of soil). In a rice paddy in China, soil OC ranged between 1-3.5 % dry weight (Wang et al., 1999).

The net CH_4 fluxes from Ka`au crater are unlikely to be influenced by PAR. On day 278, PAR was 403 µE and the net methane emission was 57 mg(CH_4) m^{-2} day^{-1}. A week later, PAR was 103 µE and the net CH_4 emission was 52 mg(CH_4) m^{-2} day^{-1}. In

theory, variation in PAR can change stomatal conductance which can increase or decrease net methane emission through plant mediated CH_4 transport or oxygenation of the rhizosphere. Here, methane emissions remained constant in the honohono meadow under two significantly (74%) different PAR levels.

4.2.3 Water Table Level (WTL) Influence on Net Methane Emissions

It has been previously demonstrated that temperature, soil chemical composition and photosynthetic activity are unlikely to affect net methane emissions in Ka`au crater. This suggests that the WTL may be the most important parameter regulating methane emissions from the Ka`au crater wetland.

To estimate the influence of the water table level on net methane emissions, CH_4 emissions data from the fixed chamber site (in the honohono meadow) were compared with the water table level data from the same location. Fig. 21 clearly indicates that methane emission is related to water table level height. However, higher or lower methane fluxes do not occur as soon as the water table level rises or drops. From day 285 to day 299, methane emissions increased steadily from 52 to 146 mg m^{-2} day^{-1} before decreasing to 94 mg m^{-2} day^{-1} on day 306. On the other hand, the water table level increased by 19 cm from day 278 to 292, and then steadily decreased by 13 cm for the next 11 days. This indicates that a rising water table level over a long enough period (here 13 days) is followed by increasing CH_4 emission rates. On the other hand, a continuous water level decline is followed by decreasing CH_4 emission rates (Fig. 21). Research in subarctic mire has shown that water table level was the most important variable controlling net methane emissions (Öquist and Svensson, 2002). Similarly, in the

honohono meadow of Ka`au crater, the WTL is most likely the main parameter controlling the magnitude of methane emissions.

The WTL fluctuated in the same manner at the two monitoring sites but one station measured a slightly higher WTL relative to the other one (i.e., 0.15 m). Field observations also indicated that parts of the study site were wetter than others probably because of micro-topographic variations. Therefore, the differences in net CH_4 emissions between plant communities may reflect in part the relative difference in WTL between the vegetation patterns studied. With these data, it is not possible to assess if the different net CH_4 flux recorded between the vegetation patterns is due exclusively to the vegetation or to the WTL. It is likely that both of these factors influence net CH_4 emissions.

Methane emissions do not immediately increase after and increase in WTL. The flux recorded one week after the WTL rise was comparable to the one recorded a week before (57 on day 278 v.s 52 mg m^{-2} day^{-1} on day 285). However, larger net methane emissions were recorded on day 292, two weeks after the water table level started to rise. This suggests that methane emissions react to water level fluctuations after a delay. Methane emissions on day 285 reflect the steady low water table level recorded from day 271 to 277 and the larger methane flux recorded on day 292 reflect the increasing water table from day 278 to 285. Fig. 21 indicates that net CH_4 emission peaks ~1 week after the WTL has risen to its maximum value. There a 3 possible explanations for the lag time between water level fluctuations and the methane flux.

Hypothesis 1: Delay in Methanogenic Activity

Methane emission from wetland soils reflects the balance between methanogenesis in anoxic zones and methanotrophy in oxic zones (Bodegom et al., 2001). Flooding of the soil induces an increase in methanogenic activity and a decline in methanotrophic activity because the oxidized zone of the soil shrinks (Le Mer and Roger, 2001). Increasing water levels decrease the rate of oxygen diffusion through the soil. Eventually, the consumption of oxygen in the soil becomes greater than the atmospheric re-supply. The soil can then become anaerobic allowing communities of methanogens to grow, multiply and convert a fresh organic matter supply into CH_4. Yet, increasing methanogenic activities may not happen as soon as anaerobic conditions develop in the soil. It may rather happen after a delay, provided that the water level remains high enough for a sufficient period to prevent diffusion of oxygen through the soil. Therefore, the delay observed between the rise of the WTL and the increase in methane emissions may reflect the time needed for the methanogenic activity to increase. For each soil incubation performed under anaerobic conditions, the CH_4 generation potential magnitude is proportional to the amount of methanogens present at the soil surface at the time of sampling, and does not reflect potential growth of the methanogenic community. If the CH_4 generation potential remains low after flooding of the soil and increases significantly after 7 days, the lag time between water table level fluctuations and the net methane emissions response may be explained in terms of methanogenic activity. A positive correlation (R^2=0.57, Fig. 22) was found between methane generation potential and water table level in the honohono meadow. This indicates that water table level also regulates surface methane generation potential. Fig. 21 shows that the surface methane

generation potential reacts rapidly to WTL fluctuations. Indeed, the highest CH_4 generation potential ($1*10^{-3}$ mg(CH_4)/g/day) was recorded on day 292, just 1 day after the water table reached its highest level (day 291, 1.13 m). A week later, the CH_4 generation potential dropped by 82% while the water table level declined by 10 cm. Therefore, the lag time between the water table fluctuations and the net methane flux response does not reflect the time needed for the methanogenic population to become active. Fig. 21 also suggests that the methanogenic population can survive under non-optimal conditions for a short period of time (i.e., with low water table level and high oxygen levels) and reactivate rapidly as soon as anaerobic conditions return.

Hypothesis 2: Persistence of methanotrophic activity

The lag time between WTL fluctuations and the net methane emission response may be also explained in terms of methanotrophic activity. The methanotrophic activity may not decrease or increase immediately after a rise or decline in water table level. The 7-day delay between the highest water table level (day 292) and the highest net methane flux (day 299) recorded may be explained because, on day 292, the methanotrophic community was still oxidizing most of the methane produced at depth. On the other hand, on day 299, the methanotrophic activity may have decreased allowing more methane to be released to the atmosphere. This hypothesis implies that soil oxygen levels may still have been high enough to support the methanotrophs on day 292 when the water table was highest. However, on day 299, the oxygen levels may have dropped to critical levels preventing the methanotrophic community to operate at their optimal potential. Methanotrophic activity is related to the methane oxidation rate constants shown in Table 7. High oxidation rate constants indicate high activities and reciprocally. If the lag time

between the WTL fluctuations and the net methane emission response is due to persistent methanotrophic activity, Fig. 21 should show that variation in WTL influence the methane oxidation rates. Instead, Fig.21 indicates that this is unlikely as the CH_4 oxidation rate constants did not change dramatically in response to WTL. A comparison of the net CH_4 emissions and CH_4 oxidation potentials suggest that methanotrophic activity increases with increasing CH_4 concentrations (Fig.21). This observation is consistent with the results from the soil incubations performed under different CH_4 concentrations in the laboratory. On the other hand, methane oxidation potentials may be reduced by decreasing CH_4 concentrations in the oxic part of the soil column (Kettunen et al., 1999). Overall, it seems that methanotrophic bacteria are much less affected by WTL fluctuations than are methanogens and cannot explain the delay.

Hypothesis 3: Rate of Methane Diffusion

The dynamic balance between CH_4 production, oxidation and transport rate from peat to the atmosphere regulates net CH_4 fluxes from wetlands (Kettunen et al., 1999). The last hypothesis that may explain the lag time required for net methane emissions to react to water table level fluctuations is the diffusion rate of CH_4 through the soil. It has been previously demonstrated that methane generation potential responds almost instantly to water table level fluctuations. However, the methane produced may not be instantaneously released to the atmosphere. By collecting peat profiles in two boreal mires, Kettunen at al, (1999) found that maximal methane production occurred 15 to 20 cm below the soil surface. It is assumed here, that maximal CH_4 generation occurs 20 cm below the soil surface in Ka`au crater. The lag time for CH_4 to diffuse through 20 cm of

soil may explain why net methane emissions are delayed. The diffusion time of a gas through any medium is given by the following equation:

$$t = \frac{X^2}{k}$$

where, X is the distance traveled by the gas through the medium (i.e., 20cm), k is the gas diffusion coefficient and t is the time required for the gas to travel trough 20cm of soil. The gas diffusion coefficient of methane through a dry soil with a porosity of 20% is given by the following equation (Rolston and Moldrup, 2002):

$$Dp = Do \times \Phi^2 \left(\frac{\varepsilon}{\Phi} \right)^{2+\frac{3}{b}}$$

where D_p is the diffusion coefficient of CH_4 through the soil, Do is the diffusion coefficient of CH_4 through air (0.21 $cm^2\ s^{-1}$) Φ is the soil porosity (assumed to be 0.2), ε is the air filled porosity and b is the water retention parameter. If the soil is completely dry the soil porosity equals the air filled porosity and ε/Φ is equal to 1. Therefore, only D_O and the porosity of the soil are needed to calculate the diffusion coefficient of CH_4. The diffusion of CH_4 through a dry soil with a 20% porosity is $8.4*10^{-3}$ $cm^2\ s^{-1}$. Therefore, the time needed for a molecule of CH_4 to diffuse through 20 cm of soil is 13 hours. With 10% soil porosity, the diffusion time is 2.2 days. These diffusion times are likely to be longer in Ka`au crater soils as it was assumed here that the soil is completely dry. This is obviously not the case in Ka`au crater. Diffusion through water is much slower. The time needed for CH_4 to diffuse through the soil is a plausible reason for the lag time between the WTL fluctuations and the net methane flux response observed in this study.

4.2.4 Methane Emissions and Precipitation

Water table variations are primarily driven by precipitation and surface drainage. In Ka`au crater the water table shows seasonal variations with lowest water table during the period of high evaporation and low rainfall through summer. In addition, there are short-term variations in water table after rain showers. During a rain event, provided that its magnitude is significant, water infiltrates through the soil, coats soil particles and fills soil pores. When all the soil pores are waterlogged the water table level starts to rise. Therefore, substantial precipitation events lead to a rise in water table level after a delay. On the contrary, summer droughts induce low water table levels because of high evaporation and low rainfall. Water table level was found to be the main environmental parameter regulating net CH_4 emissions in Ka`au crater. Because precipitation is the main factor affecting the water table level net CH_4 emissions will be correlated to precipitation, particularly with the average precipitation over week-long time scales.

Fig. 22 shows that this year was the second driest year for the Palolo Valley in the past half-century (1982 was the drier). In addition, rainfall has considerably decreased for the past 15 years in the valley and, by correlation, in Ka`au crater. Consequently, net CH_4 emission from the wetland may have significantly decreased in the past 15 years. There is a consensus among General Circulation Models (GMCs) that precipitation in Hawaii is likely to decrease by 73 mm per year with doubled atmospheric carbon dioxide levels (IPCC, 2001). Therefore, both changing vegetation and decreasing precipitation are likely to reduce the net CH_4 flux escaping the Ka`au crater wetland during this century.

Table 10. Daily average net methane emissions for the five vegetation patterns in Ka`au crater. Single measurement in `ohi`a scrub and ti thicket. Units: metric tons(CH_4) yr^{-1}

Vegetation Pattern	Average Daily Emissions
Honohono Meadow	0.5 ± 0.2
Sedge Meadow	0.4 ± 0.2
Strawberry Guava Canopy	0.07 ± 0.1
`Ohi`a Scrub	4.0
Ti Thicket	0.9
Overall Flux from Ka`au Crater	6 ± 0.3

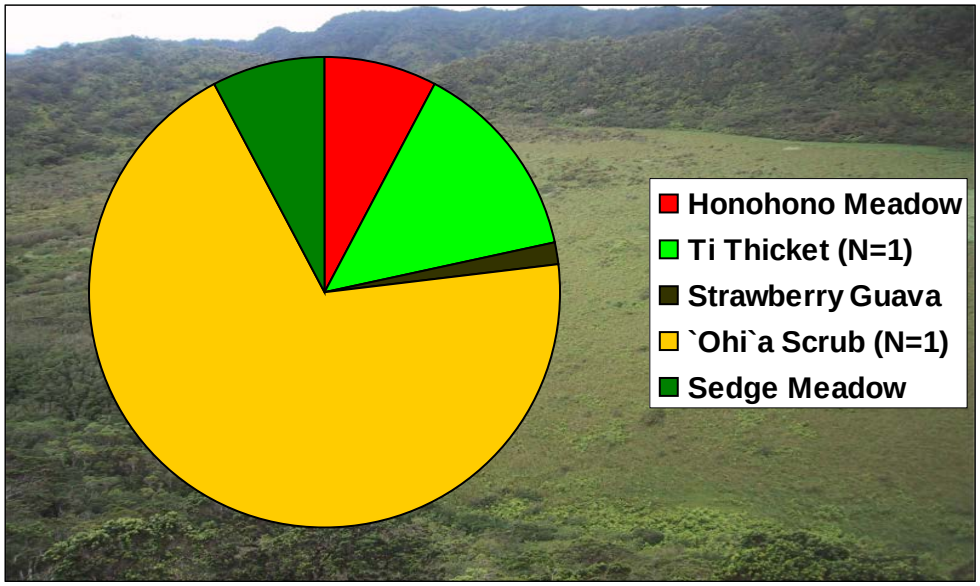

Figure 19. Contribution of each vegetation pattern to the overall CH_4 emissions from the Ka`au crater wetland

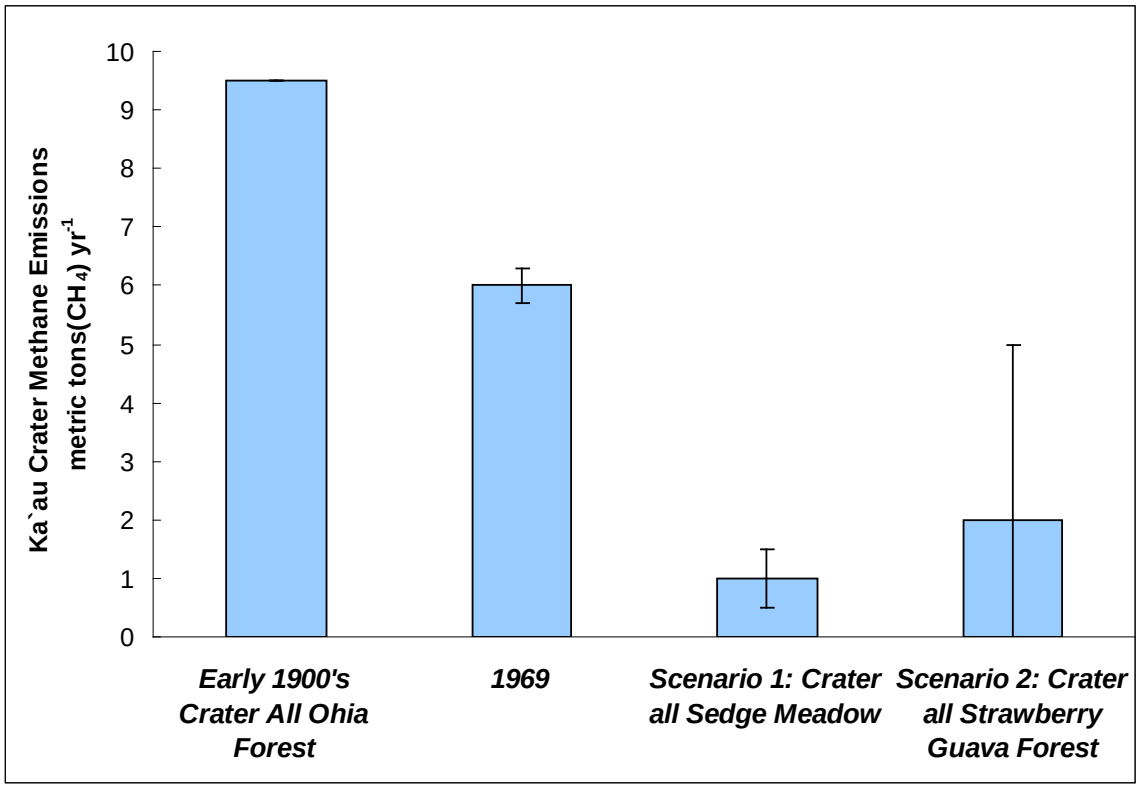

Figure 20. Past and future net CH_4 emissions from the Ka`au Crater wetland
Scenario 1: Early 1900's, Ka`au crater is entirely covered by the `ohi`a forest
Scenario 2: Emissions based on vegetation areas approximation from 1969
Future scenario 1: the sedge meadow covers the entire crater
Future scenario 2: the strawberry guava covers the entire crater

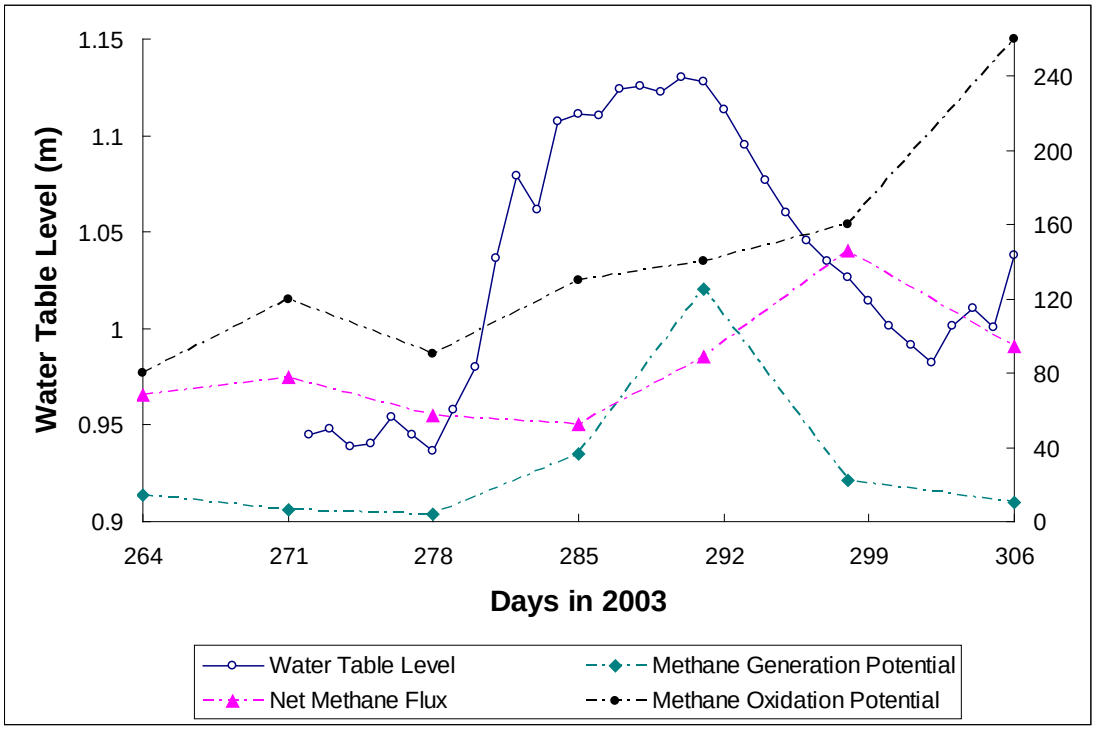

Figure 21. Net CH_4 emission, surface CH_4 generation and oxidation potential response to WTL fluctuations. The continuous blue line is the WTL (in meters), the dashed pink line the net methane flux (mg m^{-2} day^{-1}), green dashed line the surface methane generation potential (mg g(dry soil)$^{-1}$ day^{-1}) and the dashed black line the methane oxidation rate constants (hr^{-1} g(dry soil)$^{-1}$. Net methane flux peaks a week after the WTL has risen to its maximum value, while the surface generation potential reacts more rapidly. Conversely, methane oxidation rate constants are less affected by WTL fluctuations, responding possibly only to higher methane emission.

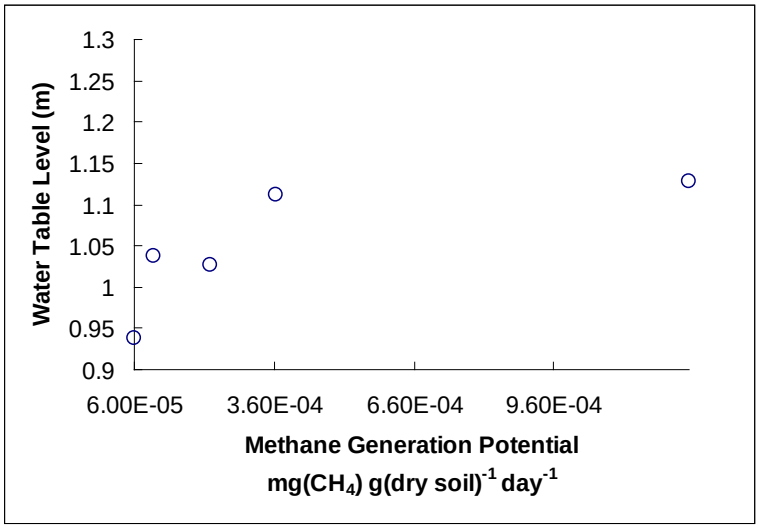

Figure 22. Correlation between honohono meadow water table level and methane generation potential

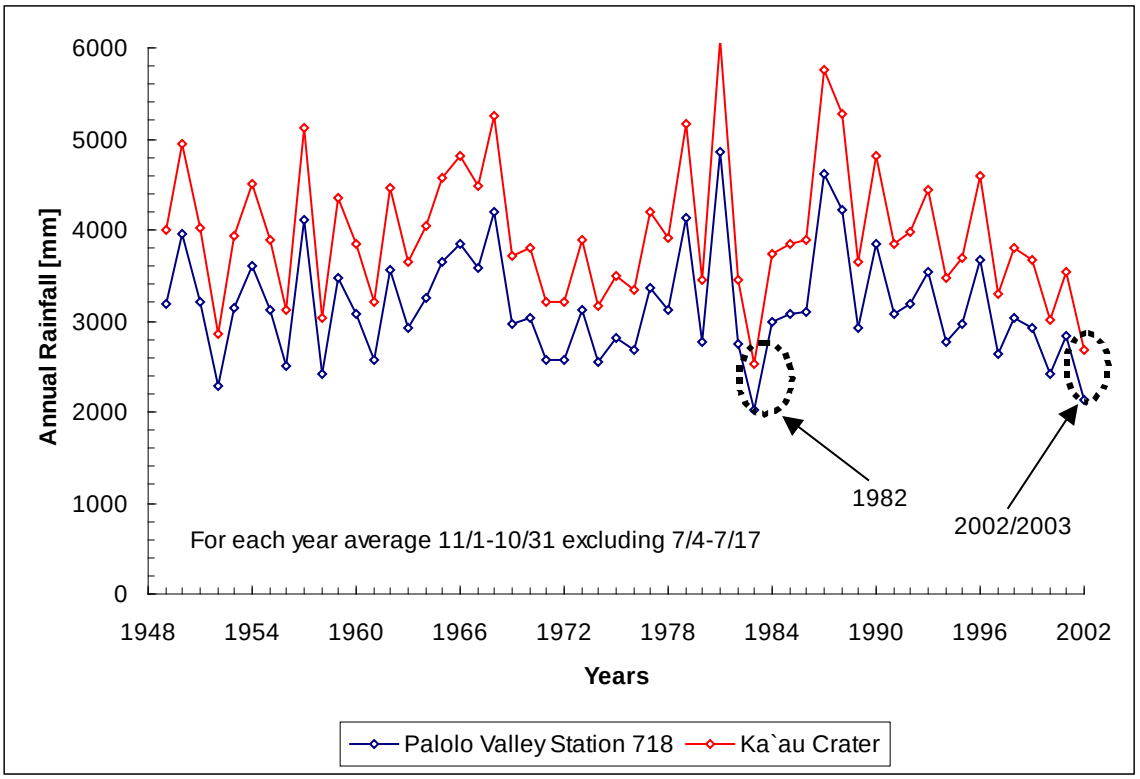

Figure 23. Precipitation in Palolo Valley and Ka`au Crater since 1949. Ka`au crater precipitation was estimated using the Palolo Valley-Ka`au Crater rainfall relation derived in section 3.2. In the Palolo Valley, precipitation was averaged each year using data from November 1st to October 31st excluding July 4th to July 17th. No data is available for this period as both rain gauges were out of service from July 4th to July 17th 2003.

5. CONCLUSIONS

This research provides a first look at the methane flux dynamics in Ka`au crater, a wetland where methane biogeochemistry had not been examined before.

It has been demonstrated that: 1) The Ka`au crater wetland was a net source of methane to the atmosphere throughout the sampling period. Net methane emissions differed significantly between the five vegetation patterns of the crater. The `ohi`a scrub, which covered the second largest area of the crater after the sedge meadow, was the most important contributor to the overall methane flux.

2) Both methanogenic and methanotrophic potential activities were recorded and varied between the vegetation patterns. Also, the net methane fluxes of the vegetation patterns studied fluctuated as the surface methane generation potentials did.

3) PAR and net methane emissions are unlikely to be correlated and the temperature fluctuations in the crater are too small to considerably affect methane generation kinetics. Furthermore, the soil organic carbon and nitrogen contents were similar in the sedge meadow, honohono meadow and strawberry guava canopy, which indicates that the different net methane emissions recorded between these vegetation patterns are not due to differences in the organic matter availability in the soil.

4) The WTL is the most important parameter regulating methane emissions in the honohono meadow of Ka`au Crater. Net methane emission is expected to depend on the thickness of the oxidized part of the soil and thus on the height of the water table. This assumption was verified as net methane emissions correlate with water table level fluctuations over a 6 weeks experimental period in the honohono meadow. Field observations and data comparison between the two water table monitoring sites suggest

that the WTL does vary throughout the study area. Consequently, the net methane emission variations observed between the vegetation patterns studied may reflect the relative difference in WTL between the plant communities or the different plant themselves. The lack of multiple time-series measurements prevented an assessment of whether plant communities or varying WTL was the most important parameter affecting the net methane fluxes in different vegetation patterns.

5) The 7-day delay between the water table level peak and the net methane emission maximum value is likely to be a consequence of gas diffusion through the soil.

6) Net methane emissions may have considerably decreased over the last century as a result of changing vegetation patterns. In the future, both changes in vegetation and decreasing precipitation may induce a lower methane flux from the Ka`au crater wetland.

This study, however, suffers from major limitations, including the lack of static chamber experiments in large portions of the wetland and the lack of plant-associated methane flux measurements for all vegetation patterns. In the future, more static chamber incubations could be done in the patterns where only one experiment was performed (i.e., `ohi`a scrub and ti thicket) to better estimate the average emission from these sites. Several plant-associated flux measurements covering a larger area of the Ka`au crater wetland could be performed to differentiate the influence of vegetation relative to water table level. All this possible future work would quantify the overall net methane emission from the crater more accurately.

References

Armstrong, R.W., (1983) “Atlas of Hawai`i." University of Hawai`i Press, Honolulu

Bartlett, K.B., Harriss, R.C. (1993) Review and assessment of methane emissions from wetlands. *Chemosphere* 26, 261-320.

Bodegom, P., Stams, F., Mollema, L., Boeke, S., Leffelaar, P. (2001) Methane oxidation and the competition for oxygen in the rice rhizosphere. *Applied Environmental Microbiology* 67, 3586-3597.

Chang, T.C., Yang, S.S. (2003) Methane emission from wetlands in Taiwan. *Atmospheric Environment* 37, 4551-4558.

Heilman, M.A., Carlton, R.G., (2001) Methane oxidation associated with submersed vascular macrophytes and its impact on plant diffusive methane flux. *Biogeochemistry* 52, 207-224.

Hotchkiss, S., Juvik, J.O., (1999) A late-Quaternary pollen record from Ka`au crater, O`ahu, Hawai`i. *Quaternary Research* 52, 115-128.

Intergovernmental Panel on Climate Change (IPCC), (2000) Emission scenarios, Special report of the Intergovernmental Panel on Climate Change, Cambridge Univ. Press, Cambridge UK, available at http://www.ipcc.ch/pub/pub.htm

Intergovernmental Panel on Climate Change (IPCC), (2001) Climate Change 2001: Working Group 1: The scientific basis, Cambridge Univ. Press, Cambridge UK, available at http://www.grida.no/climate/ipcc_tar/wgl/134.htm

Intergovernmental Panel on Climate Change (IPCC), (2001) Climate Change 2001: Synthesis Report, Cambridge Univ. Press, Cambridge UK, available at http://www.grida.no/climate/ipcc_tar/slides/07.19.htm

Kennedy, E. (1975) Ka`au Crater: A study of plant patterns in an Hawaiian bog. Unpublished M.A dissertation, University of Hawai`i.

Kettunen, A., Kaitala, V., Lehtinen, A., Lohila, A., Alm, J., Silvola, J., Martikainen, P.J., (1999) Methane production and oxidation potentials in relation to water table fluctuations in two boreal mires. *Soil Biology and Biochemistry* 31, 1741-1749.

King, G.M., Roslev, P., Skovgaard, H., (1990) Distribution and rate of methane oxidation in sediments of the Florida Everglades. *Applied and Environmental Microbiology* 56: 2902-2911

Le Mer, J., Roger, P., (2001) Production, oxidation, emission and consumption of methane by soils : A review. *Eur. J. Soil Biol* 37, 25-50.

Mac Donald, G.A., Abbott, A.T., Peterson, F.L., (1983) *Volcanoes in the Sea.* University of Hawai`i Press, Honolulu

Mackenzie, F.T., (1998) *Our Changing Planet. An introduction to earth system science and global environmental change*. Second Edition, Prentice Hall.

Matthews, E., Fung, I., (1987) Methane emissions from natural wetlands: Global distribution, area and environmental characteristics of sources. *Global Biogeochemical Cycles.* 1, 61-86.

Milich, L., (1999) The role of methane in global warming: where might mitigation strategies be focused? *Global Environmental Change* 9, 179-201.

Miyajima, T., Wada, E., Hanba, Y.T., Vijarnsorn, P., (1997) Anaerobic mineralization of indigenous organic matters and methanogenesis in tropical wetland soils. *Geochimica and Cosmochimica Acta* 61, 3739-3751.

National Climatic Data Center (NCDC) (2003), Palolo Valley Station #718 Climatic Data available at
http://www4.ncdc.noaa.gov/cgi/win/wwcgi.dll?wwDI~StnSrch~StnID~20023515

Öquist, M.G., Svensson, B.H., (2002) Vascular plants as regulators of methane emissions from a subarctic mire ecosystem. *Journal of Geophysical Research* 107, ACL 10-1, 10-10.

Prather, M.J., Derwent, R., Ehhalt, D., Fraser, P., Sanhueza, E., Zhou, X., (1995) Other trace gases and atmospheric chemistry. pp 373 in *Biogeochemistry: An Analysis of Global Change.* Academic Press, San Diego.

Rolston, D.E., Moldrup, P., (2002) The soil gas phase :4.3 Gas Diffusivity in Dane, J.H. and C. Topp (eds.) Methods of Soil Analysis. Part 4, SSAS Book Ser.5, Madison, WI pp 1113-1139.

Sahagion, D., Melack, J., (1996) Global wetland distribution and functional characterization: Trace gases and the hydrologic cycle. Available at
http://gaim.unh.edu/Products/Reports_2/report2.pdf

Schlesinger, W.H., (1997) *Biogeochemistry: An Analysis of Global Change.* Academic Press, San Diego

Severinghaus, J.P., Sowers, T., Brook, E.J., Alley, R.B., Benders, M.L., (1998) Timing of abrupt climate change at the end of the Younger Dryas interval from thermally fractionated gases in polar ice. *Nature* 391, 141-146.

Schütz, L., Schröeder, P., Rennenberg, H., (1991). Role of plants in regulating the methane flux to the atmosphere. pp.239. In Schlesinger, W.H., *Biogeochemistry: An Analysis of Global Change.* Academic Press, San Diego.

Wang, B., Xu, Y., Wang, Z., Li, Z., Ding, Y., Guo, Y., (1999) Methane production potentials of twenty-eight rice soils in China. *Biol. Fertil. Soils* 29:74-80

Appendix I. Rhizospheric oxidation

Methanotrophic oxidation associated with root tissues from the species *Scirpus Validus* (Honohono Meadow) and *Cladium Leptostachyum* (Sedge Meadow) is shown in the following figure. Three scenarios were observed: Scenarios 1 & 2 show the expected oxidation of methane over time, while scenario 3, which was the most common observation, show an unexpected net CH_4 increase over time. Methane concentrations in the control bottle (i.e., with just CH_4 and tap water) remained constant over time, indicating that the serum bottles sealed with butyl rubber stoppers and aluminum crimp seals were not leaking. The unexpected CH_4 increase in scenario 3 may be due to the development of anoxic conditions in the incubation bottles leading to methane generation. The lag time observed in scenario 2 before detecting decreasing methane concentrations could not be explained. A better way to perform this experiment would be to use serum bottles with a larger volume (i.e., 150 mL instead of 25 mL) and to regulate O_2 concentrations in the bottles. Overall, scenarios 1 & 2 indicate that some methanotrophic bacteria are associated with plant roots of the species *Scirpus Validus* and *Cladium Leptostachyum.*

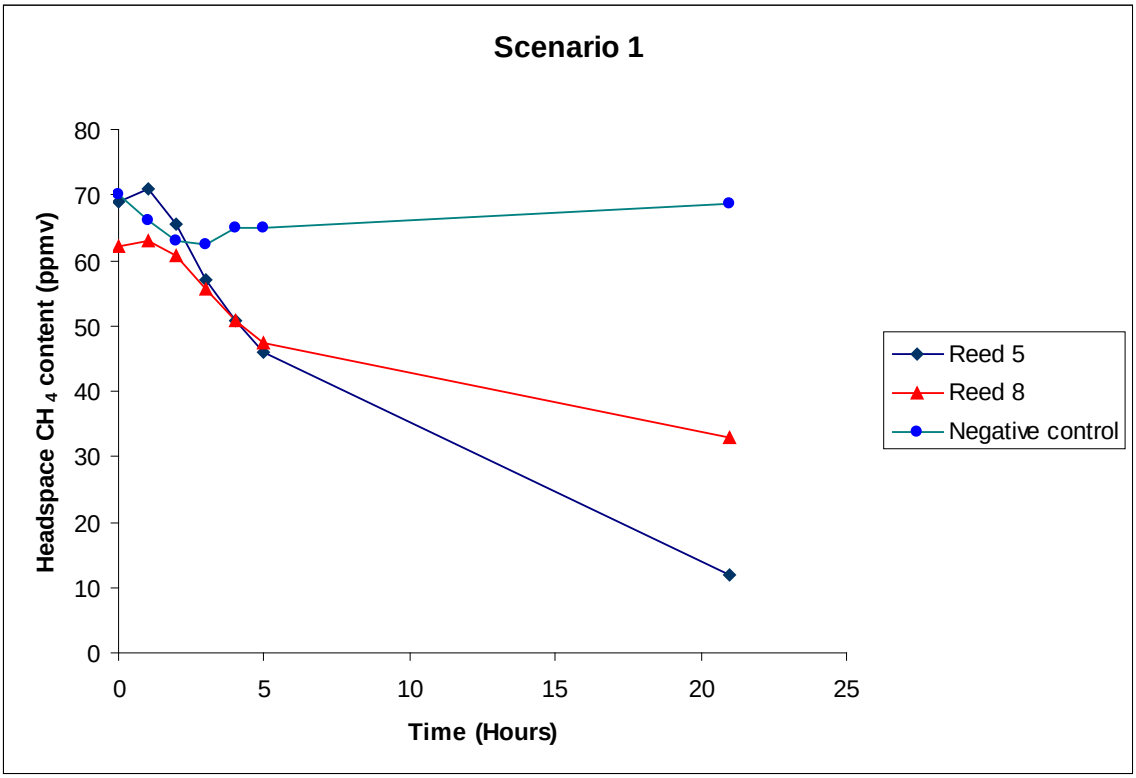
Scenario 1
Headspace CH 4 content (ppmv)
80
70
60
50
40
30
20
10
0
0
5
10
15
20
25
Time (Hours)
Reed 5
Reed 8
Negative control

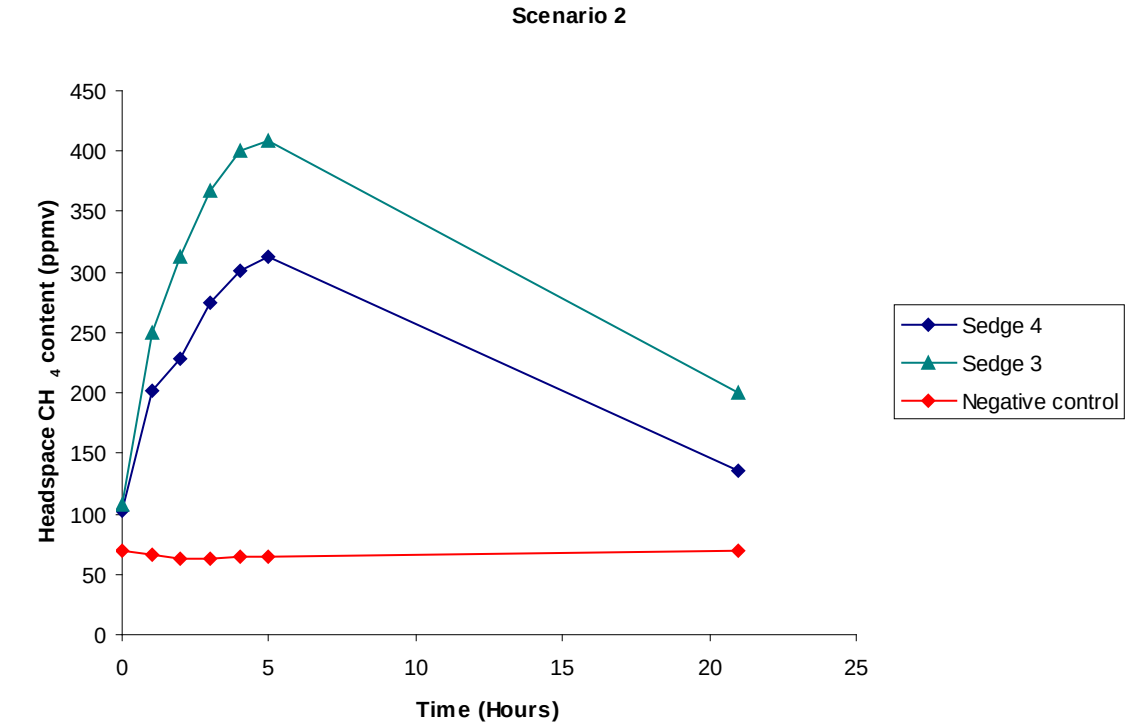
Scenario 2
Headspace CH 4 content (ppmv)
450
400
350
300
250
200
150
100
50
0
0
5
10
15
20
25
Time (Hours)
Sedge 4
Sedge 3
Negative control

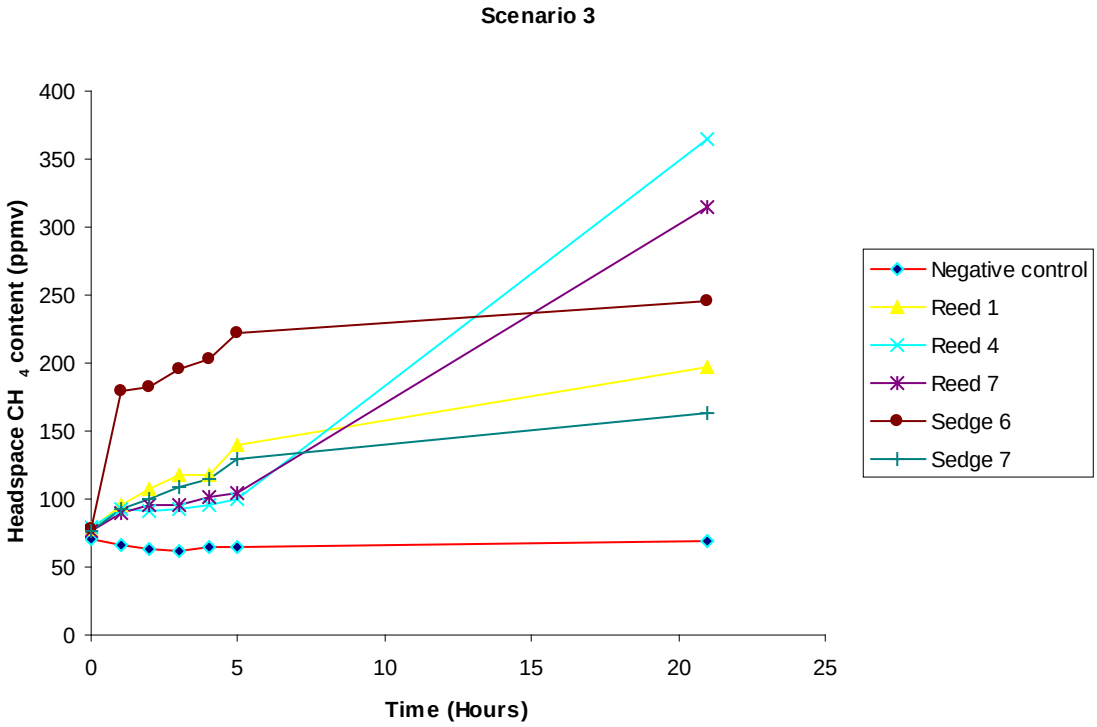
Scenario 3
Headspace CH 4 content (ppmv)
400
350
300
250
200
150
100
50
0
0
5
10
15
20
25
Time (Hours)
Negative control
Reed 1
Reed 4
Reed 7
Sedge 6
Sedge 7

Appendix II. Daily average PAR throughout the experimental period